

Horn loudspeakers

9

CHAPTER OUTLINE

Part XXVIII: Horn drive units	407
9.1 Introduction	407
9.2 Electro-mechano-acoustical circuit	408
9.3 Reference efficiency.....	410
9.4 Frequency response	412
9.5 Examples of horn calculations	416
Part XXIX: Horns	417
9.6 General description	417
9.7 Possible profiles	417
9.8 Mouth size.....	419
9.9 Infinite parabolic horn	419
9.10 Infinite conical horn	421
9.11 Infinite exponential horn	422
9.12 Infinite hyperbolic horn (hypex)	425
9.13 Finite horns.....	428
9.14 Bends in horns	435
9.15 Cross-sectional shapes.....	438
9.16 Materials.....	438

PART XXVIII: HORN DRIVE UNITS

9.1 INTRODUCTION

Horn loudspeakers usually consist of an electrodynamic drive unit coupled to a horn. When well designed, the large end of the horn, called the “mouth,” has an area sufficiently large to radiate sound efficiently at the lowest frequency desired. The small end of the horn, called the “throat,” has an area selected to match the acoustic impedance of the drive unit and to produce as little nonlinear distortion of the acoustic signal as possible.

Horn loudspeakers are in widespread use in cinemas, theaters, concert halls, stadiums, and arenas where large acoustic powers must be radiated and where control of the direction of sound radiation is desired. The efficiency of radiation of sound from one side of a well-designed direct-radiator loudspeaker was shown in Chapters 6 and 7 to be typically less than 1%. By comparison, the efficiency of radiation from a horn loudspeaker usually lies between 10% and 50%.

The principal disadvantages of horn loudspeakers compared with the direct-radiator loudspeakers are higher cost and larger size.

Before proceeding with an analysis of the horn loudspeaker, it should be mentioned again that the radiating efficiency of a direct-radiator loudspeaker can be increased at low frequencies by mounting several units side by side in a single baffle. The mutual interaction among the radiating units serves to increase the radiation resistance of each unit substantially. For example, two identical direct-radiator loudspeakers very near each other in an infinitely large plane baffle, and vibrating in phase, will produce four times the intensity on the principal axis as will one of them alone.

Direct-radiator loudspeakers used in multiple often are not as satisfactory at high frequencies as one horn loudspeaker because of the difficulty of obtaining uniform phase conditions from different direct-radiator diaphragms. That is to say, the conditions of vibration of a loudspeaker cone are complex, so that normal variations in the uniformity of cones result in substantial differences in the phases of the radiated signals of different cones at high frequencies. A very irregular and unpredictable response curve and directivity pattern result.

This problem does not arise with a horn where only a single drive unit is employed. When two or more drive units are used to drive a single horn, the frequency range in which the response curve is not adversely affected by the multiplicity of drive units is that where the diaphragms vibrate in one phase.

9.2 ELECTRO-MECHANO-ACOUSTICAL CIRCUIT [1]

The drive unit for a horn loudspeaker is essentially a small direct-radiator loudspeaker that couples to the throat of a flaring horn as shown in Fig. 9.1. In the next part we shall discuss the characteristics of the horn itself. In this section we restrict ourselves to that part of the frequency range where the complex mechanical impedance Z_{MT} looking into the throat of a horn is a pure resistance:

$$Z_{MT} = \frac{1}{Y_{MT}} = \rho_0 c S_T \text{ N} \cdot \text{s/m} \quad (9.1)$$

where

ρ_0 is density of air in kg/m^3

c is velocity of sound in m/s

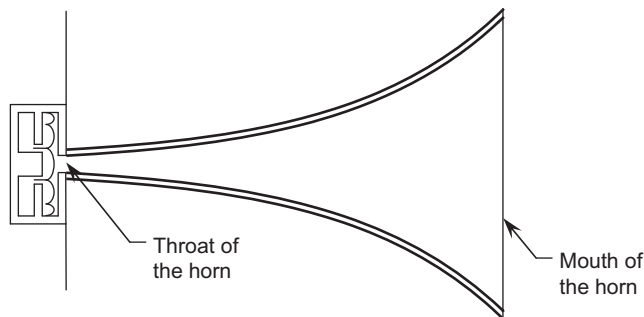


FIG. 9.1 Cross section of a simple horn loudspeaker with an exponential cross section.

For this design, the radius of the throat is 0.1, the radius of the mouth 1.7, and the length 5.0 (arbitrary units).

$\rho_0 c = 406$ raysl at 22°C and 10^5 Pa ambient pressure

S_T is area of the throat in m^2

Y_{MT} is mechanical admittance at the throat of the horn in $\text{m} \cdot \text{N}^{-1} \cdot \text{s}^{-1}$

A cross-sectional drawing of a compression drive unit for a horn loudspeaker is shown in Fig. 9.2. It has a diaphragm and voice coil with a total mass M_{MD} , a mechanical compliance C_{MS} , and a mechanical resistance $R_{MS} = 1/G_{MS}$. The quantity G_{MS} is the mechanical conductance of the diaphragm in $\text{m} \cdot \text{N}^{-1} \cdot \text{s}^{-1}$.

Behind the diaphragm is a back cavity that is usually filled with a soft acoustical material. At low frequencies this space acts as a compliance C_{MB} which can be lumped in with the compliance of the diaphragm. At high frequencies the reactance of this space becomes small so that the space behind the diaphragm becomes a mechanical radiation resistance $R_{MB} = 1/G_{MB}$ with a magnitude equal to that given in Eq. (9.1). This resistance combines with the mechanical radiation resistance of the throat, and the diaphragm must develop power both to its front and its back. Obviously, any power developed behind the diaphragm is wasted, and at high frequencies this sometimes becomes as much as one-half of the total generated acoustic power.

In front of the diaphragm there is an air space or front cavity with compliance C_{M1} . At low frequencies the air in this space behaves like an incompressible fluid, that is, ωC_{M1} is small, and all the air displaced by the diaphragm passes into the throat of the horn. At high frequencies the mechanical reactance of this air space becomes sufficiently low (i.e., the air becomes compressible) so that all the air displaced by the diaphragm does not pass into the throat of the horn.

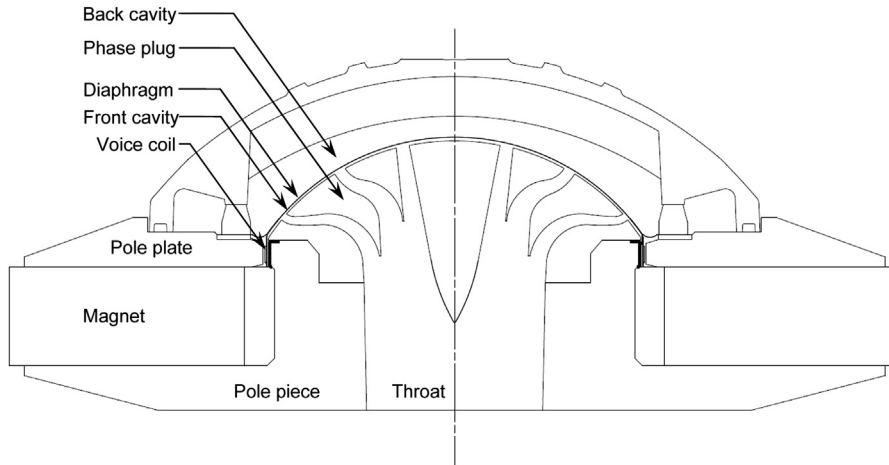


FIG. 9.2 Cross section of a horn compression drive unit.

The diaphragm couples to the throat of the horn through a small cavity with a mechanical compliance C_{M1} . Note that in this design, the annular channels within the phase plug meet the front cavity at nodal points so as to suppress the normal modes which would otherwise occur [19]. Such modes would produce a somewhat uneven frequency response.

Courtesy of Celestion.

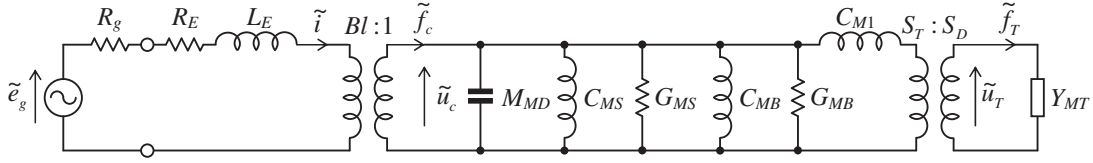


FIG. 9.3 Electro-mechano-acoustical analogous circuit of the admittance type for the drive unit.

To derive this, we assume that the mechanical impedance at the horn throat is $\rho_0 c S_T$, that is, the mechanical admittance is $Y_{MT} = 1/(\rho_0 c S_T)$.

The voice coil has an electrical resistance R_E and inductance L_E . As stated above, Y_{MT} is the mechanical admittance at the throat of the horn.

By inspection, we draw the admittance-type analogous circuit shown in Fig. 9.3. In this circuit forces “flow” *through* the elements, and the velocity “drops” *across* them. The generator open-circuit voltage and resistance are \tilde{e}_g and R_g . The electric current is \tilde{i} ; the linear velocity of the voice coil and diaphragm is \tilde{u}_c ; the linear velocity of the air at the throat of the horn is \tilde{u}_T ; and the force at the throat of the horn is \tilde{f}_T . As before, the area of the diaphragm is S_D , and that of the throat is S_T .

9.3 REFERENCE EFFICIENCY

In the middle-frequency range many approximations usually can be made to simplify the analogous circuit of Fig. 9.3. Because the drive unit is very small, the mass of the diaphragm and the voice coil M_{MD} is very small. This in turn usually means that the compliance of the suspension C_{MS} is large in order to keep the resonance frequency low. Also, the conductance of the suspension G_{MS} usually is large, and the reactance ωC_{M1} is small. Hence, in this frequency range, the circuit reduces essentially to that of Fig. 9.4a, where the conductance behind the diaphragm is

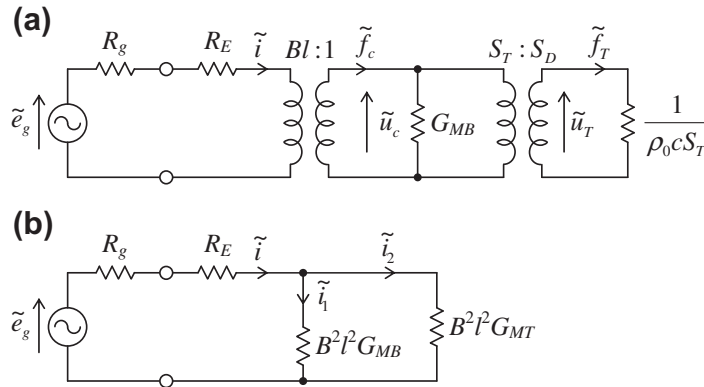


FIG. 9.4 Simplified analogous circuits of the admittance type for the drive unit in the region where the motion of the diaphragm is resistance-controlled by the horn.

$$G_{MB} \equiv \frac{1}{\rho_0 c S_D} \quad \text{m} \cdot \text{N}^{-1} \cdot \text{s}^{-1} \quad (9.2)$$

With the area-changing and electromechanical transformers removed, we get Fig. 9.4b, where the radiation conductance at the throat is

$$G_{MT} \equiv \frac{S_T}{\rho_0 c S_D^2} \quad \text{m} \cdot \text{N}^{-1} \cdot \text{s}^{-1} \quad (9.3)$$

As before, S_T is the area of the throat and S_D is the area of the diaphragm in m^2 . We have assumed here that the cavity behind the diaphragm in this frequency range is nearly perfectly absorbing, which may not always be true. Usually, however, this circuit is valid over a considerable frequency range because of the heavy damping provided by the conductance of the horn G_{MT} . Also, G_{MT} usually is smaller than G_{MB} so that most of the power supplied by the diaphragm goes into the horn.

Solution of Fig. 9.4b gives us

$$\tilde{i}_2 = \frac{G_{MB}}{G_{MB} + G_{MT}} \tilde{i} \quad (9.4)$$

Assuming that the output resistance R_g of the generator is small compared with the coil resistance R_E of the drive unit, the total electrical power supplied from the generator is

$$\text{Total power supplied} = \left| \frac{\tilde{i}}{\sqrt{2}} \right|^2 \left(R_E + B^2 l^2 \frac{G_{MB} G_{MT}}{G_{MB} + G_{MT}} \right) \quad (9.5)$$

Using the solution of Eq. (9.4), the reference efficiency E_{ff} is equal to the power delivered to the horn,

$$\left| \tilde{i}_2 / \sqrt{2} \right|^2 B^2 l^2 G_{MT},$$

times 100 divided by the total power supplied:

$$E_{ff} = \frac{(G_{MB} / (G_{MB} + G_{MT}))^2 B^2 l^2 G_{MT}}{R_E + B^2 l^2 G_{MB} G_{MT} / (G_{MB} + G_{MT})} \times 100 \quad (9.6)$$

From Eqs. (9.2), (9.3), and (9.6) we get

$$E_{ff} = \frac{100 B^2 l^2 (S_T / S_D)}{(1 + S_T / S_D) ((B^2 l^2 + S_D \rho_0 c R_E) (S_T / S_D) + S_D \rho_0 c R_E)} \quad (9.7)$$

or, in terms of Thiele–Small parameters,

$$E_{ff} = \frac{100 (S_T / S_D) S_{DC}}{(1 + S_T / S_D) ((S_{DC} + \omega_S Q_{ES} V_{AS}) (S_T / S_D) + \omega_S Q_{ES} V_{AS})} \quad (9.8)$$

where we have used Eqs. (6.27) and (6.30) for the Bl factor. We note that the value of G_{MT} , and hence the ratio S_T / S_D would seem to need to be large for high efficiency. However, if S_T / S_D becomes too large, reference to Fig. 9.4b shows that too much power will be dissipated in G_{MB} and the efficiency

will be low. In order to optimize the efficiency, let us now differentiate the above with respect to (S_T/S_D) and equate the result to zero. Hence maximum efficiency occurs when

$$\frac{S_T}{S_D} = \sqrt{\frac{S_D \rho_0 c R_E}{B^2 l^2 + S_D \rho_0 c R_E}} = \sqrt{\frac{\omega_S Q_{ES} V_{AS}}{S_{DC} + \omega_S Q_{ES} V_{AS}}} \quad (9.9)$$

so that the maximum efficiency is

$$E_{ff}(\max) = \frac{100 B^2 l^2}{\left(\sqrt{B^2 l^2 + S_D \rho_0 c R_E} + \sqrt{S_D \rho_0 c R_E} \right)^2} \quad (9.10)$$

which can also be given in terms of Thiele–Small parameters:

$$E_{ff}(\max) = \frac{100 S_{DC}}{(\sqrt{S_{DC} + \omega_S Q_{ES} V_{AS}} + \sqrt{\omega_S Q_{ES} V_{AS}})^2} \quad (9.11)$$

To increase the efficiency further, it is seen from Eq. (9.10) that the length l of the wire on the voice coil should be increased as much as possible without altering electrical resistance R_E . Within given space limitations, this can be done by winding the voice coil from wire with a rectangular cross section rather than with a circular cross section. This means that the voice-coil mass will be increased. Increasing l further will demand wire of larger cross section which will require a larger air gap, with a corresponding reduction in B or increase in magnet size. Also, the voice coil must not become too large as its mass will limit the high-frequency response.

9.4 FREQUENCY RESPONSE

The frequency response of a complete horn loudspeaker, in the range where the throat impedance of the horn is a resistance as given by Eq. (9.1), is determined by solution of the circuit of Fig. 9.3. A horn-loaded drive unit behaves very differently from a direct radiator. The diaphragm of a direct-radiator loudspeaker is *mass-controlled* because a flat on-axis response is given at frequencies where the acceleration of the diaphragm is constant. Because the velocity decreases with frequency, so does the radiated power for $\omega > c/a$, but this is compensated for by an increasingly narrow directivity pattern, which is how the flat on-axis response is maintained. By contrast, a horn has a fairly constant directivity pattern over its operating frequency range. Hence, for a flat frequency response, the radiated power must also be constant, which can only be achieved if the velocity is constant. Hence the diaphragm of horn-loaded drive unit is *resistance-controlled*. For purposes of analysis, we shall divide the frequency range into three parts, A, B, and C, as shown in Fig. 9.5.

Mid-frequency range. In the mid-frequency range, designated as B in Fig. 9.5, the response is equal to the reference efficiency given by Eq. (9.8). Here, the response is “flat” with frequency, and, for the usual high-frequency units used in auditoriums with 300 Hz cutoff frequencies, the flat region extends from a little above 500 to a little below 3000 Hz. In this region the velocity of the diaphragm is constant with frequency, rather than decreasing in inverse proportion to frequency as was the case for a direct-radiator loudspeaker.

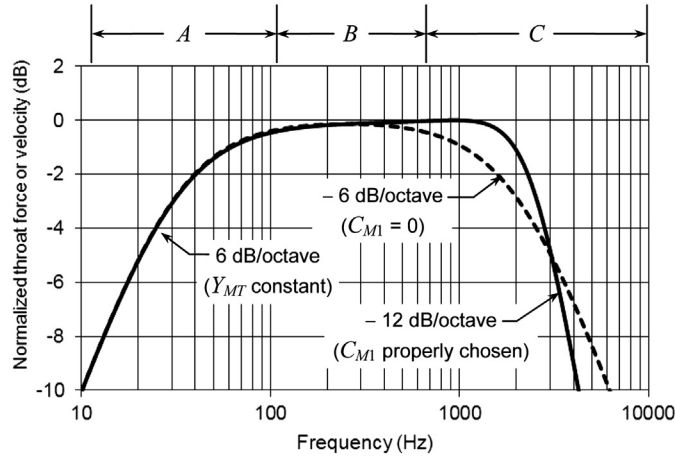


FIG. 9.5 Normalized frequency response of the mechanical force \tilde{f}_T or velocity \tilde{u}_T at the throat of a horn drive unit, in the frequency region where the mechanical impedance at the throat is a pure resistance $\rho_0 c S_T$.

The ordinate is a logarithmic scale, proportional to decibels.

Resonance frequency. It is apparent from Fig. 9.3 that since ωC_{M1} is small, zero reactance will occur at the frequency where

$$f_0 = \frac{1}{2\pi \sqrt{M_{MD}(C_{MS}C_{MB}/(C_{MS} + C_{MB}))}} \quad (9.12)$$

In practice, this resonance usually is located in the middle of region B of Fig. 9.5 and is heavily damped by the conductance G_{MT} , so that the velocity of the diaphragm is resistance-controlled.

Low frequencies. At frequencies well below the resonance frequency the response will drop off 6 dB for each octave decrease in frequency if the throat impedance is a resistance as given by Eq. (9.1). This case is shown as region A in Fig. 9.5.

Let us simplify Fig. 9.3 so that it is valid only for the low-frequency region, well below the resonance of the diaphragm. Then the inductance L_E , the mass M_{MD} , the compliance C_{M1} and the conductances G_{MS} and G_{MB} may all be dropped from the circuit, giving us Fig. 9.6.

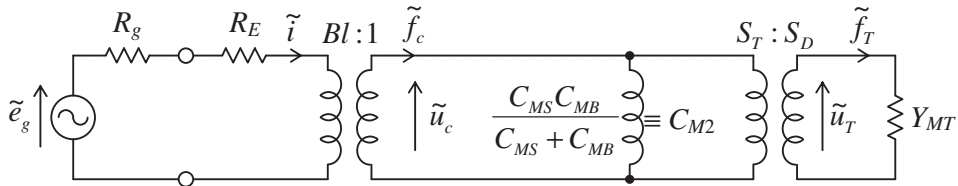


FIG. 9.6 Analogous circuit for a horn drive unit in the region where the diaphragm would be stiffness-controlled if the horn admittance were infinite.

The actual value of the mechanical admittance of the horn at the throat is Z_{MT} .

Assuming the throat admittance of the horn is a pure conductance as given by Eq. (9.3), the frequency at which the frequency response is 3 dB down is given in terms of the Thiele–Small parameters by

$$\omega_L = \left(1 + \frac{V_{AS}}{V_B}\right) \frac{\omega_S Q_{ES} S_{DC}}{S_{DC} + (1 + S_D/S_T) \omega_S Q_{ES} V_{AS}} \quad (9.13)$$

where V_B is the volume of the back cavity. In practice, however, the throat impedance Z_{MT} of the horn near the lowest frequency at which one wishes to radiate sound is *not* a pure resistance. Hence, region A needs more careful study. Solving for the mechanical admittance at the diaphragm of the drive unit yields

$$Y_{Mc} = \frac{\tilde{u}_c}{\tilde{f}_c} = \frac{j\omega C_{M2} (S_T/S_D)^2 Y_{MT}}{j\omega C_{M2} + (S_T/S_D)^2 Y_{MT}} \quad (9.14)$$

where

$$C_{M2} = \frac{C_{MS} C_{MB}}{C_{MS} + C_{MB}} \quad (9.15)$$

and Y_{MT} is mechanical admittance at the throat of the horn with area S_T . The mechanical impedance at the diaphragm of the drive unit is the reciprocal of Y_{Mc} ,

$$Z_{Mc} = \frac{\tilde{f}_c}{\tilde{u}_c} = \left(\frac{S_D}{S_T}\right)^2 Z_{MT} - j \frac{1}{\omega C_{M2}} \quad (9.16)$$

where $Z_{MT} = 1/Y_{MT}$ is mechanical impedance at the throat of the horn with area S_T .

As we shall show in the next part, the mechanical impedance at the throat of ordinary types of horn at the lower end of the useful frequency range is equal to a mechanical resistance in series with a negative compliance. That is to say,

$$Z_{MT} \equiv \mathbf{R}_{MT} + j \frac{1}{\omega C_{MT}} \quad (9.17)$$

The bold \mathbf{R}_{MT} indicates that this resistance varies with frequency. Usually, its variation is between zero at very low frequencies and $\rho_0 c S_T$ [as given by Eq. (9.1)] at some frequency in region A of Fig. 9.5. Hence, the admittance $Y_{MT} = 1/Z_{MT}$ is a resistance in series with a negative mass reactance. In the frequency range where this is true, therefore, the reactive part of the impedance Z_{Mc} can be canceled out by letting [see Eqs. (9.16) and (9.17)]

$$\frac{S_D^2}{S_T^2} \frac{1}{C_{MT}} = \frac{1}{C_{M2}} = \left(\frac{1}{C_{MB}} + \frac{1}{C_{MS}} \right) \quad (9.18)$$

Then,

$$Z_{Mc} = \mathbf{R}_{MT} \left(\frac{S_D}{S_T} \right)^2 \equiv \frac{1}{\mathbf{G}_{Mc}} \quad (9.19)$$

where G_{Mc} is the acoustic conductance of the throat of the horn at low frequencies transformed to the diaphragm.

The efficiency for frequencies where the approximate circuit of Fig. 9.6 holds, and where the conditions of Eq. (9.18) are met, is

$$E_{ff} = \frac{100B^2l^2G_{Mc}}{R_E + B^2l^2G_{Mc}} \quad (9.20)$$

assuming $R_g \gg R_E$. The conductance G_{Mc} usually varies from “infinity” at very low frequencies down to $S_T/(S_D^2\rho_0c)$ at some frequency in region A of Fig. 9.5.

High frequencies. At very high frequencies, the response is limited principally by the combined mass of the diaphragm and the voice coil M_{MD} . If the compliance C_{M1} of the front cavity were zero, the response would drop off at the rate of 6 dB per octave (see region C of Fig. 9.5). It is possible to choose C_{M1} to resonate with M_{MD} at a frequency that extends the response upward beyond where it would extend if it were limited by M_{MD} alone. We can understand this situation by deriving a circuit valid for the higher frequencies as shown in Fig. 9.7. It is seen that a damped anti-resonance occurs at a selected high frequency ω_U , which is given in terms of the Thiele–Small parameters of the drive unit by

$$\omega_U = \omega_S \sqrt{\frac{V_{AS}}{V_F} \left\{ 1 + \frac{S_T}{S_D} \left(1 + \frac{S_{DC}}{\omega_S Q_{ES} V_{AS}} \right) \right\}} \quad (9.21)$$

with a Q_U value of

$$Q_U = \omega_U \left\{ \frac{S_{TC}}{V_F} + \omega_S \left(\frac{1}{Q_{ES}} + \frac{\omega_S V_{AS}}{S_{DC}} \right) \right\}^{-1} \quad (9.22)$$

where V_F is the volume of the front cavity. Above this resonance frequency, the response drops off 12 dB for each octave increase in frequency (see region C of Fig. 9.5).

Because the principal diaphragm resonance [Eq. (9.12)] is highly damped by the throat resistance of the horn, it is possible to extend the region of flat response of a drive unit over a range of four octaves by proper choice of C_{M1} at higher frequencies and by meeting the conditions of Eq. (9.18) at lower frequencies.

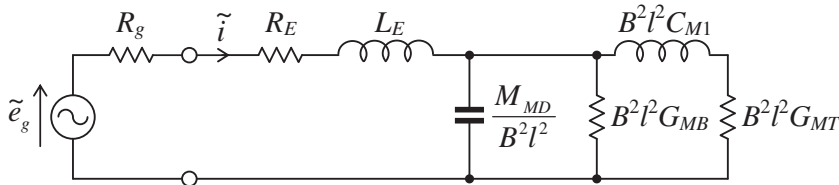


FIG. 9.7 Analogous circuit for a horn drive unit at high frequencies where the diaphragm mass reactance is much larger than its compliance reactance.

9.5 EXAMPLES OF HORN CALCULATIONS

Example 9.1. Find the maximum efficiency of a 2-inch theater horn drive unit designed to operate in the frequency range above 500 Hz with the following Thiele–Small parameters:

$$\begin{aligned} R_E &= 6.4 \, \Omega \\ Q_{ES} &= 0.8 \\ f_S &= 250 \, \text{Hz} \\ S_D &= 13.2 \, \text{cm}^2 \\ V_{AS} &= 0.1 \, \text{L}. \end{aligned}$$

Solution. From Eq. (9.9) the optimum throat area is

$$\begin{aligned} S_T &= 13.2 \times 10^{-4} \times \sqrt{\frac{2 \times 3.14 \times 250 \times 0.8 \times 0.1 \times 10^{-3}}{13.2 \times 10^{-4} \times 348.8 + 2 \times 3.14 \times 250 \times 0.8 \times 0.1 \times 10^{-3}}} \\ &= 6.11 \, \text{cm}^2 \end{aligned}$$

which from Eq. (9.11) gives a maximum efficiency of

$$\begin{aligned} E_{ff}(\text{max}) &= \frac{100 S_D c}{\left(\sqrt{13.2 \times 10^{-4} \times 348.8 + 2 \times 3.14 \times 250 \times 0.8 \times 0.1 \times 10^{-3}} + \sqrt{2 \times 3.14 \times 250 \times 0.8 \times 0.1 \times 10^{-3}} \right)^2} \\ &= 36.7\% \end{aligned}$$

Example 9.2. In order to extend the high-frequency response of the previous example, reduce the throat area to $S_T = 0.66 \, \text{cm}^2$ ($S_T/S_D = 0.05$) and recalculate the efficiency. Also determine the upper resonance frequency and the Q of the resonance, as well as the theoretical lower cutoff frequency that would be obtained with an infinite horn of low cutoff frequency and a 0.1 L back cavity (i.e., $V_B = V_{AS}$).

Solution. Then we obtain the efficiency from Eq. (9.8), which gives

$$\begin{aligned} E_{ff} &= \frac{100 \times 0.05 \times 13.2 \times 10^{-1} \times 348.8}{(1 + 0.05)((13.2 \times 10^{-1} \times 348.8 + 2 \times 3.14 \times 250 \times 0.8 \times 0.1) \times 0.05 + 2 \times 3.14 \times 250 \times 0.8 \times 0.1)} \\ &= 14.2\% \end{aligned}$$

which is still quite good. If we set the depth d of the front cavity to $d = 1 \, \text{mm}$ so that $V_F \approx d S_D = 1.32 \, \text{cm}^3$, we obtain the high-frequency resonance from Eq. (9.21), which gives

$$\begin{aligned} f_U &= 250 \sqrt{\frac{0.1 \times 10^{-3}}{1 \times 10^{-3} \times 13.2 \times 10^{-4}} \left\{ 1 + 0.05 \times \left(1 + \frac{13.2 \times 10^{-4} \times 348.8}{2 \times 3.14 \times 250 \times 0.8 \times 0.1 \times 10^{-3}} \right) \right\}} \\ &= 2.42 \, \text{kHz} \end{aligned}$$

Using Eq. (9.22) we obtain a Q value of

$$Q_U = 2 \times 3.14 \times 2420 \times \left\{ \frac{0.66 \times 10^{-4} \times 348.8}{10^{-3} \times 13.2 \times 10^{-4}} + 2 \times 3.14 \times 250 \left(\frac{1}{0.8} + \frac{2 \times 3.14 \times 250 \times 0.1 \times 10^{-3}}{13.2 \times 10^{-4} \times 348.8} \right) \right\}^{-1}$$

$$= 0.762$$

which is fairly optimal for a flat frequency-response with a smooth roll-off. Finally, from Eq. (9.13) we obtain the following lower cut-off frequency with an ideal infinite horn:

$$f_L = \frac{1}{2 \times 3.14} (1 + 1) \frac{2 \times 3.14 \times 250 \times 0.8 \times 13.2 \times 10^{-4} \times 348.8}{13.2 \times 10^{-4} \times 348.8 + (1 + 20) \times 2 \times 3.14 \times 250 \times 0.8 \times 0.1 \times 10^{-3}}$$

$$= 59.4 \text{ Hz}$$

Of course this is unrealistic in practice as the lower cutoff frequency is more likely to be determined by the characteristics of the horn, which we shall examine in the next section. The full frequency response is plotted in Fig. 9.5.

PART XXIX: HORNS

9.6 GENERAL DESCRIPTION

A horn is in effect an acoustic transformer. It transforms a small-area diaphragm into a large-area diaphragm without the difficulties of cone resonances discussed in Part XX. A large-area diaphragm has a radiation impedance that is more nearly resistive over the desired frequency range than is the radiation impedance for a small-area diaphragm (see Fig. 4.35). As a result, more power is radiated at low frequencies for a given volume velocity of air. A horn is also a directivity controlling device, which radiates over an angle defined by the flare angle of the mouth.

In designing a horn for a particular application we usually wish to select the parameters so as to radiate the maximum amount of acoustic power over the desired frequency range with suitably low nonlinear distortion. Once we have stated the frequency range, tolerable distortion, and desired radiated power, we can choose the drive unit and then proceed to calculate the throat and the mouth diameters and the length and shape of the horn.

9.7 POSSIBLE PROFILES [2]

When it comes to considering various horn profiles, there are only a limited number with exact solutions. For a start, an exact solution relies upon a coordinate system which leads to a separable wave equation. In other words, the coordinate system must be orthogonal, having coordinate surfaces which all meet at right angles. In Part V we presented solutions to the three-dimensional Helmholtz wave equation in three such coordinate systems, namely, rectangular, cylindrical, and spherical. Generally, cylindrical coordinates lead to parabolic horns (with two parallel and two non-parallel side walls), while spherical coordinates lead to conical horns.

There only a few other three-dimensional orthogonal coordinate systems which lead to practical horn profiles. Of these are spheroidal coordinates, which come in two flavors: prolate and oblate. Although they are too complicated to deal with in this text, they are worth mentioning. Spheroidal coordinates are constructed from overlapping families of ellipses and hyperbolas, which share two focal points. If the ellipses are rotated about an axis passing through the focal points, they become prolate spheroids (cigar shaped) and we have a prolate-spheroidal coordinate system. Then any one of the rotated hyperbolas can be chosen as a horn profile. Such a profile looks parabolic near the throat but becomes more conical as the distance from the throat increases. Similarly, if the ellipses are rotated about an axis passing between the two focal points, they become oblate spheroids (flying saucer shaped) and we have an oblate-spheroidal coordinate system. Again, any one of the rotated hyperbolas can be chosen as a horn profile [3]. In this case, however, the profile looks hyperbolic near the throat but becomes more conical as the distance from the throat increases. However, spheroidal wave functions, [4,20] unlike Bessel and Legendre functions, are not frequency independent. The fact that a whole series of harmonics must be calculated at each frequency step somewhat complicates the analysis. Ellipsoidal coordinates lead to similar horn profiles, but with cross-sections that are not circular.

Some other three-dimensional coordinate systems are simply two-dimensional systems translated through parallel planes. For example, elliptical-cylindrical coordinates are formed by translating the ellipses and hyperbolas of the spheroidal system. From this we can form horn profiles having two straight parallel walls and two curved walls which are hyperbolas. Again, we have the problem that the resulting Mathieu functions [4] are not frequency independent.

A rigorous treatment of a horn profile would involve solving the wave equation in three-dimensions with the correct boundary conditions at the throat, walls and mouth, but the analysis would be somewhat complicated. It is much simpler if we can reduce the wave equation down to one dimension by assuming that pressure variations over the cross-section of the horn are minimal. In practice, the errors produced by such an assumption are fairly small. We have already introduced Webster's equation, [21] Eq. (2.27), which is one-dimensional, but allows for a number of different functions $S(x)$ to describe the variation of cross-sectional area S with distance x along its length. However, this equation assumes that the wave front does not change shape as it progresses along the length of the horn, otherwise it is not truly one-dimensional. In the case of a parabolic horn (with two parallel walls and two non-parallel) or conical horn, this assumption is generally true. However, we shall also consider exponential and hyperbolic horns in which case the wave front starts off substantially planar near the throat and becomes more curved as it progresses along the length of the horn. As a result, the infinite horn exhibits an abrupt cutoff frequency below which no power is transmitted. However, for a finite horn, the errors produced by this one-dimensional assumption are not too bad. It should be noted that there is no orthogonal coordinate system for an exponential or hyperbolic horn that leads to a separable wave equation with an exact solution, but proposals have been made to improve Webster's one-dimensional theory which include recasting it [5], applying expansions [6] or correction factors [7,8], and smoothing the cutoff discontinuity with a complex wave number [9].

First we shall consider infinite horns, as these provide the simplest solutions for the throat impedance and hence radiated power under idealized conditions. If the horn is a number of wavelengths long and if the mouth circumference is larger than the wavelength, we may call it "infinite" in length. This simplification leads to equations that are easy to understand and are generally useful in design. Then we shall develop 2-port transmission matrices for finite horns, which can be used as part of an overall loudspeaker system design. Our analysis will be limited to parabolic, conical, exponential, and hyperbolic horns.

For a horn to be a satisfactory transformer, its cross-sectional area near the throat end should increase gradually with axial distance x . If it does, the transformation ratio remains reasonably constant with frequency over a wide range. Exponential and hyperbolic horns are closer to this ideal, but the more gradual cutoff of a conical horn makes it easier to integrate into a loudspeaker system when used as a high-frequency unit or tweeter. The parabolic horn is often used in reverse as a transmission line because it is the easiest to construct.

We already mentioned that the directivity is largely defined by the flare angle at the mouth. This is certainly the case for parabolic and conical horns when the wavelength is smaller than the diameter of the mouth. The mouth of a conical horn behaves somewhat like a spherical cap in a sphere because it produces spherical waves which are largely confined within the angle of the apex of the cone at high frequencies. A conical horn may not necessarily have a circular cross-section though. A rectangular cross-section enables different angles of dispersion in the horizontal and vertical planes. It also produces a smoother on-axis response. Pulsating spherical and rectangular caps in spheres are discussed in Example 9.4 and covered in detail in Sec. 12.7. The high-frequency directivity factor is

$$Q(f) = \frac{4\pi R^2}{S_M} \quad (9.23)$$

where R is the radius at the mouth and S_M is the area of the mouth. In the case of a rectangular cone, the area is given by Eq. (12.69). Unfortunately, exponential and hyperbolic horns produce a more planar wave in the middle of the flare at high frequencies, resulting in a somewhat narrower directivity pattern. Multiple horns, or “multi-cell” horns are often used to mitigate this effect. They may either comprise multiple horns with each having its own drive unit or horns with a common drive unit. Another option is to use a hybrid exponential/conical horn [10].

9.8 MOUTH SIZE

The large end (mouth) of the horn should have a circumference large enough so that the radiation impedance is nearly resistive over the desired frequency range. Reference to Fig. 4.35 shows that this will be true for $ka > 1$: that is, $C/\lambda > 1$, where C is the circumference of the mouth of the horn and λ is the wavelength of the lowest tone that it is desired to radiate. If the mouth of the horn is not circular but square, it will behave in nearly the same way, as far as radiated power is concerned, for equal mouth areas. Hence, for good design, the mouth circumference C or mouth area S_M ,

$$C = 2\sqrt{\pi S_M} > \lambda \quad (9.24)$$

where λ is the longest wavelength of sound that is to be radiated efficiently.

9.9 INFINITE PARABOLIC HORN [11]

Theoretical considerations. A parabolic horn can either have a rectangular cross section with two parallel straight walls and two non-parallel straight walls, or a circular cross section with a curved wall following a parabola. The former gives more accurate results using the one-dimensional wave equation

and is easier to construct, but in the figures we shall use the latter for convenience. The equation describing the cross-sectional area $S(x)$ as a function of the distance x along the axis is

$$S(x) = S_T x / x_T \quad (9.25)$$

where S_T is the area of the throat, which is located at a distance $x = x_T$ ahead of the apex at $x = 0$. In the steady state, the Helmholtz equation for the parabolic horn is

$$\left(\frac{\partial^2}{\partial x^2} + \frac{1}{x} \frac{\partial}{\partial x} + k^2 \right) \tilde{p}(x) = 0 \quad (9.26)$$

where

$$k = \frac{2\pi}{\lambda} = \frac{\omega}{c} \quad (9.27)$$

and

\tilde{p} is harmonically varying sound pressure at a point along the length of the horn in Pa. (It is assumed that the pressure is uniform across the cross section of the horn.)

c is speed of sound in m/s.

x is distance along the length of the horn from the apex in m.

x_T is distance from the apex to the throat in m.

S_T is cross-sectional area of the throat in m^2 .

S is cross-sectional area at x in m^2 .

The general solution for the pressure in a parabolic horn of any length is

$$\tilde{p}(x) = \tilde{p}_+ H_0^{(2)}(kx) + \tilde{p}_- H_0^{(1)}(kx) \quad (9.28)$$

where \tilde{p}_+ denotes the pressure amplitude of the forward traveling wave and \tilde{p}_- that of the backwards traveling wave. The tilde replaces the factor $e^{j\omega t}$. Using Eq. (2.87), the velocity is given by

$$\begin{aligned} \tilde{u}(x) &= -\frac{1}{jk\rho_0 c} \frac{\partial}{\partial x} \tilde{p}(x) \\ &= \frac{1}{j\rho_0 c} \left(\tilde{p}_+ H_1^{(2)}(kx) + \tilde{p}_- H_1^{(1)}(kx) \right) \end{aligned} \quad (9.29)$$

Throat impedance. Noting that in an infinite horn there are no reflections from the mouth, we set $\tilde{p}_- = 0$ in order to obtain the acoustic throat impedance, which is the ratio of the pressure \tilde{p} to the volume velocity \tilde{U} at $x = x_T$, so that

$$\begin{aligned} Z_{AT} &= \frac{\tilde{p}(x_T)}{\tilde{U}(x_T)} = \frac{\tilde{p}(x_T)}{S_T \tilde{u}(x_T)} = j \frac{\rho_0 c}{S_T} \frac{H_0^{(2)}(kx_T)}{H_1^{(2)}(kx_T)} \\ &= \frac{\rho_0 c}{S_T} \left(\frac{2}{\pi k x_T (J_1^2(kx_T) + Y_1^2(kx_T))} + j \frac{J_0(kx_T) J_1(kx_T) + Y_0(kx_T) Y_1(kx_T)}{J_1^2(kx_T) + Y_1^2(kx_T)} \right) \text{N} \cdot \text{s} / \text{m}^5 \end{aligned} \quad (9.30)$$

where we have used the relationships of Eqs. (75) and (111) from Appendix II. This is the same as the radiation impedance of an infinitely long pulsating cylinder of radius x_T . If we equate the real and imaginary parts of the impedance, we find that the *cutoff frequency* occurs at $kx_T = 0.268$, which we shall designate f_c , where

$$f_c = \frac{0.268c}{2\pi x_T} \quad (9.31)$$

The throat impedance of an infinite parabolic horn is plotted in Fig. 9.9.

9.10 INFINITE CONICAL HORN

Theoretical considerations. The equation describing the cross-sectional area $S(x)$ as a function of the distance x along the axis is

$$S(x) = S_T(x/x_T)^2 \quad (9.32)$$

where S_T is the area of the throat, which is located at a distance $x = x_T$ ahead of the apex at $x = 0$. In the steady state, the Helmholtz equation for the conical horn is

$$\left(\frac{\partial^2}{\partial x^2} + \frac{2}{x} \frac{\partial}{\partial x} + k^2 \right) \tilde{p}(x) = 0 \quad (9.33)$$

where

$$k = \frac{2\pi}{\lambda} = \frac{\omega}{c} \quad (9.34)$$

and

\tilde{p} is harmonically varying sound pressure at a point along the length of the horn in Pa. (It is assumed that the pressure is uniform across the cross section of the horn.)

c is speed of sound in m/s.

x is distance along the length of the horn from the apex in m.

x_T is distance from the apex to the throat in m.

S_T is cross-sectional area of the throat in m^2 .

S is cross-sectional area at x in m^2 .

The general solution for the pressure in a conical horn of any length is

$$\tilde{p}(x) = \tilde{p}_+ \frac{e^{-jkx}}{x} + \tilde{p}_- \frac{e^{jkx}}{x} \quad (9.35)$$

where \tilde{p}_+ denotes the pressure amplitude of the forward traveling wave and \tilde{p}_- that of the backwards traveling wave. The tilde replaces the factor $e^{j\omega t}$. Using Eq. (2.87), the velocity is given by

$$\begin{aligned} \tilde{u}(x) &= -\frac{1}{jk\rho_0 c} \frac{\partial}{\partial x} \tilde{p}(x) \\ &= \frac{1}{\rho_0 c} \left\{ \tilde{p}_+ \left(1 - \frac{j}{kx} \right) \frac{e^{-jkx}}{x} - \tilde{p}_- \left(1 + \frac{j}{kx} \right) \frac{e^{jkx}}{x} \right\} \end{aligned} \quad (9.36)$$

Throat impedance. Noting that in an infinite horn there are no reflections from the mouth, we set $\tilde{p}_- = 0$ in order to obtain the acoustic throat impedance, which is the ratio of the pressure \tilde{p} to the volume velocity \tilde{U} at $x = x_T$, so that

$$\begin{aligned} Z_{AT} &= \frac{\tilde{p}(x_T)}{\tilde{U}(x_T)} = \frac{\tilde{p}(x_T)}{S_T \tilde{u}(x_T)} = \frac{\rho_0 c}{S_T} \frac{jkx_T}{1 + jkx_T} \\ &= \frac{\rho_0 c}{S_T} \left(\frac{k^2 x_T^2}{1 + k^2 x_T^2} + j \frac{kx_T}{1 + k^2 x_T^2} \right) \text{N} \cdot \text{s/m}^5 \end{aligned} \quad (9.37)$$

This is the same as the radiation impedance of a pulsating sphere of radius x_T . The special case of $kx_T = 1$ occurs at the *cutoff frequency*, which we shall designate f_c , where

$$f_c = \frac{c}{2\pi x_1} \quad (9.38)$$

The throat impedance of an infinite conical horn is plotted in Fig. 9.9.

9.11 INFINITE EXPONENTIAL HORN

Theoretical considerations. The equation describing the cross-sectional area $S(x)$ as a function of the distance x along the axis is

$$S(x) = S_T e^{mx} \quad (9.39)$$

where S_T is the area of the throat, which is located at $x = 0$. In the steady state, the Helmholtz equation for the exponential horn is

$$\left(\frac{\partial^2}{\partial x^2} + m \frac{\partial}{\partial x} + k^2 \right) \tilde{p}(x) = 0 \quad (9.40)$$

where

$$k = \frac{2\pi}{\lambda} = \frac{\omega}{c} \quad (9.41)$$

and

\tilde{p} is harmonically varying sound pressure at a point along the length of the horn in Pa. (It is assumed that the pressure is uniform across the cross section of the horn.)

c is speed of sound in m/s.

x is distance along the length of the horn from the throat in m.

m is flare constant in m^{-1} . Obviously, m determines the magnitude of the second term of the equation above, which expresses the rate at which the sound pressure changes with distance down the horn. If $m = 0$, Eq. (9.40) becomes the equation for propagation in a cylindrical tube, i.e., a horn with zero flare.

S_T is cross-sectional area of the throat in m^2 .

S is cross-sectional area at x in m^2 .

The general solution for the pressure in an exponential horn of any length is

$$\tilde{p}(x) = e^{-mx/2} \left(\tilde{p}_+ e^{-jkx\sqrt{1-\frac{m^2}{4k^2}}} + \tilde{p}_- e^{jkx\sqrt{1-\frac{m^2}{4k^2}}} \right) \quad (9.42)$$

where \tilde{p}_+ denotes the pressure amplitude of the forward traveling wave and \tilde{p}_- that of the backwards traveling wave. The tilde replaces the factor $e^{j\omega t}$. Using Eq. (2.87), the velocity is given by

$$\begin{aligned} \tilde{u}(x) &= -\frac{1}{jk\rho_0 c} \frac{\partial}{\partial x} \tilde{p}(x) \\ &= \frac{e^{-mx/2}}{\rho_0 c} \left\{ \tilde{p}_+ \left(\sqrt{1-\frac{m^2}{4k^2}} - j\frac{m}{2k} \right) e^{-jkx\sqrt{1-\frac{m^2}{4k^2}}} - \tilde{p}_- \left(\sqrt{1-\frac{m^2}{4k^2}} + j\frac{m}{2k} \right) e^{jkx\sqrt{1-\frac{m^2}{4k^2}}} \right\} \end{aligned} \quad (9.43)$$

Throat impedance. Noting that in an infinite horn there are no reflections from the mouth, we set $\tilde{p}_- = 0$ in order to obtain the acoustic throat admittance, which is the ratio of the volume velocity \tilde{U} to the pressure \tilde{p} at $x = x_T$, so that

$$\begin{aligned} Y_{AT} &= \frac{\tilde{U}(x_T)}{\tilde{p}(x_T)} = \frac{S_T \tilde{u}(x_T)}{\tilde{p}(x_T)} = \frac{S_T}{\rho_0 c} \left(\sqrt{1-\frac{m^2}{4k^2}} - j\frac{m}{2k} \right) \text{m}^5 \cdot \text{N}^{-1} \cdot \text{S}^{-1} \\ &= G_{AT} + jB_{AT} \end{aligned} \quad (9.44)$$

The acoustic impedance $Z_{AT} = 1/Y_{AT}$ at the throat is

$$\begin{aligned} Z_{AT} &= \frac{\rho_0 c}{S_T} \left(\sqrt{1-\frac{m^2}{4k^2}} + j\frac{m}{2k} \right) \\ &= R_{AT} + jX_{AT} \text{N} \cdot \text{s}/\text{m}^5 \end{aligned} \quad (9.45)$$

The real and imaginary parts of Z_{AT} and Y_{AT} behave alike with frequency and differ only by the magnitude $(S/\rho_0 c)^2$ and the sign of the imaginary part. Note also that, unlike with the parabolic or conical horns, this impedance is independent of the distance x along the axis of the horn. Let us see next how varying the flare constant m affects the acoustic impedance Z_{AT} .

Flare constant and throat impedance. When the flare constant m is *greater* than 4π divided by the wavelength ($m > 2k$, low frequencies), the acoustic resistance R_{AT} and the acoustic reactance X_{AT} at the throat of the horn where the area is S_T , are

$$\begin{aligned} R_{AT} &= 0 \\ X_{AT} &= \frac{\rho_0 c}{S_T} \left(\frac{m}{2k} - \sqrt{\frac{m^2}{4k^2} - 1} \right) \end{aligned} \quad (9.46)$$

When the flare constant m equals 4π divided by the wavelength, the acoustic resistance and reactance are

$$\begin{aligned} R_{AT} &= 0 \\ X_{AT} &= \frac{\rho_0 c m}{2k S_T} = \frac{\rho_0 c}{S_T} \end{aligned} \quad (9.47)$$

For all cases where m is less than 4π divided by the wavelength ($m < 2k$, high frequencies), the acoustic resistance and reactance at any point x along the horn where the cross-sectional area is S are

$$\begin{aligned} R_{AT} &= \frac{\rho_0 c}{S_T} \sqrt{1 - \frac{m^2}{4k^2}} \\ X_{AT} &= \frac{\rho_0 c m}{2k S_T} = \frac{\rho_0 c^2 m}{2\omega S_T} \equiv \frac{1}{\omega C_{AT}} \end{aligned} \quad (9.48)$$

where $C_{AT} = 2S_T/\rho_0 c^2 m$.

For very high frequencies, the reactance approaches zero and the resistance approaches $\rho_0 c/S_T$ or $\rho_0 c/S$ in general. This is also the impedance for a plane progressive sound wave in a tube of uniform cross section S .

Cutoff frequency. The special case of $m = 4\pi/\lambda$ occurs at a frequency which we shall designate f_c , where

$$f_c = \frac{mc}{4\pi} \quad (9.49)$$

This frequency f_c is called the cutoff frequency because, for frequencies lower than this, no power will be transmitted down the horn, i.e., the impedance at all positions along the horn is purely reactive [see Eq. (9.46)]. The throat impedance of an infinite exponential horn is plotted in Fig. 9.9.

To obtain the acoustic impedance at the throat of the horn in terms of the cutoff frequency, we observe that $f_c/f = m/2k$. Substituting in Eq. (9.45) yields

$$Z_{AT} = \frac{\rho_0 c}{S_T} \left(\sqrt{1 - \left(\frac{f_c}{f}\right)^2} + j \frac{f_c}{f} \right) = R_{AT} + jX_{AT} \quad (9.50)$$

where

S_T is throat area in m^2 .

$\rho_0 c$ is characteristic impedance of air in rayls.

f_c is cutoff frequency.

f is driving frequency.

Graphs of two quantities A and B that are directly proportional to the resistive and reactive parts of the acoustic impedance at the throat of an infinitely long exponential horn are shown in Fig. 9.8. The

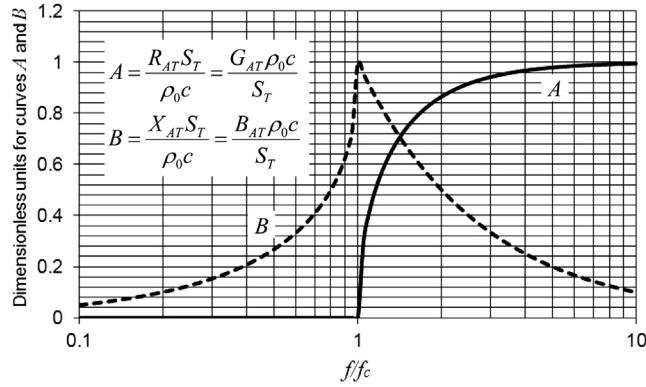


FIG. 9.8 Plot of the quantities A and B , which are defined by the relations given on the graph.

quantities A and B also are directly proportional to the real and imaginary parts of the acoustic admittance at the throat. The relations among A , B , R_{AT} , X_{AT} , G_{AT} , and B_{AT} are given on the graph. When the frequency is greater than approximately double the cutoff frequency f_c , the throat impedance is substantially resistive and very near its maximum value in magnitude.

9.12 INFINITE HYPERBOLIC HORN (HYPEX) [12]

Theoretical considerations. The equation describing the cross-sectional area $S(x)$ as a function of the distance x along the axis is

$$S(x) = S_T \left(\cosh \frac{x}{x_T} + \alpha \sinh \frac{x}{x_T} \right)^2 \quad (9.51)$$

where S_T is the area of the throat, which is located at $x = 0$ and $0 \leq \alpha \leq 1$. We can vary the parameter α in order to create any profile between hyperbolic ($\alpha = 0$) and exponential ($\alpha = 1$). In the steady state, the Helmholtz equation for the hyperbolic horn is

$$\left(\frac{\partial^2}{\partial x^2} + \frac{2}{x_T} \frac{\sinh(x/x_T) + \alpha \cosh(x/x_T)}{\cosh(x/x_T) + \alpha \sinh(x/x_T)} \cdot \frac{\partial}{\partial x} + k^2 \right) \tilde{p}(x) = 0 \quad (9.52)$$

where

$$k = \frac{2\pi}{\lambda} = \frac{\omega}{c} \quad (9.53)$$

and

\tilde{p} is harmonically varying sound pressure at a point along the length of the horn in Pa. (It is assumed that the pressure is uniform across the cross section of the horn.)

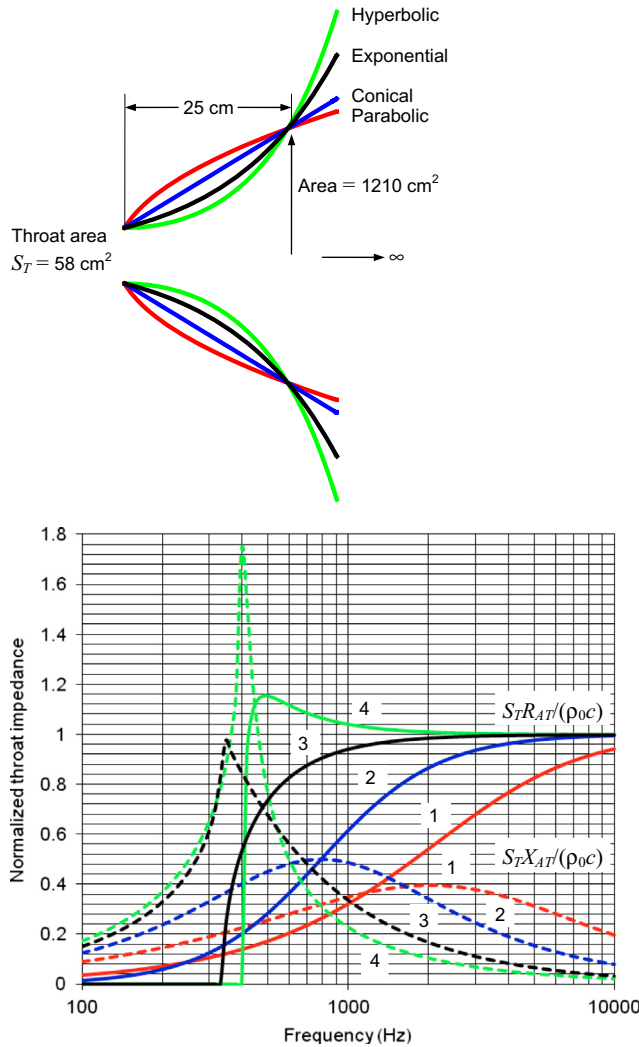


FIG. 9.9 Plot of normalized throat impedances for infinite parabolic (1), conical (2), exponential (3), and hyperbolic (4) horns using Eqs. (9.30), (9.37), (9.45), and (9.57) respectively.

Real impedances $S_T R_{AT}/(\rho_0 c)$ are represented by solid curves and the imaginary impedances $S_T X_{AT}/(\rho_0 c)$ are represented by dashed curves. The value of α for the hyperbolic horn is $\frac{1}{2}$. The cutoff frequencies of the parabolic, conical, exponential, and hyperbolic horns are 1182 Hz, 792 Hz, 337 Hz, and 399 Hz respectively.

c is speed of sound in m/s.

x_T is reference axial distance from the throat in m.

x is distance along the length of the horn from the throat in m.

α is parameter which never exceeds unity.

S_T is cross-sectional area of the throat in m^2 .

S is cross-sectional area at x in m^2 .

The general solution for the pressure in an hyperbolic horn of any length is

$$\tilde{p}(x) = \frac{1}{\cosh(x/x_T) + \alpha \sinh(x/x_T)} \left(\tilde{p}_+ e^{-jkx \sqrt{1 - \frac{1}{k^2 x_T^2}}} + \tilde{p}_- e^{jkx \sqrt{1 - \frac{1}{k^2 x_T^2}}} \right) \quad (9.54)$$

where \tilde{p}_+ denotes the pressure amplitude of the forward traveling wave and \tilde{p}_- that of the backwards traveling wave. The tilde replaces the factor $e^{j\omega t}$. Using Eq. (2.87), the velocity is given by

$$\tilde{u}(x) = -\frac{1}{jk\rho_0 c} \frac{\partial}{\partial x} \tilde{p}(x) \quad (9.55)$$

Throat impedance. Noting that in an infinite horn there are no reflections from the mouth, we set $\tilde{p}_- = 0$ in order to obtain the acoustic throat admittance, which is the ratio of the volume velocity \tilde{U} to the pressure \tilde{p} at $x = x_T$, so that

$$\begin{aligned} Y_{AT} &= \frac{\tilde{U}(x_T)}{\tilde{p}(x_T)} = \frac{S_T \tilde{u}(x_T)}{\tilde{p}(x_T)} = \frac{S_T}{\rho_0 c} \left(\sqrt{1 - \frac{1}{k^2 x_T^2}} - j \frac{\alpha}{k x_T} \right) \text{m}^5 \cdot \text{N}^{-1} \cdot \text{s}^{-1} \\ &= G_{AT} + jB_{AT} \end{aligned} \quad (9.56)$$

The acoustic impedance $Z_{AT} = 1/Y_{AT}$ at the throat is

$$\begin{aligned} Z_{AT} &= \frac{\rho_0 c}{S_T} \left(\sqrt{1 - \frac{1}{k^2 x_T^2}} - j \frac{\alpha}{k x_T} \right)^{-1} \text{N} \cdot \text{s} / \text{m}^5 \\ &= R_{AT} + jX_{AT} \end{aligned} \quad (9.57)$$

The real and imaginary parts of Z_{AT} and Y_{AT} behave alike with frequency and differ only by the magnitude $(S/\rho_0 c)^2$ and the sign of the imaginary part. Note also that like with an exponential horn, but unlike the parabolic or conical horns, this impedance is independent of the distance x along the axis of the horn.

Cutoff frequency. The special case of $x_T = \lambda/2\pi$ occurs at a frequency which we shall designate f_c , where

$$f_c = \frac{c}{2\pi x_T} \quad (9.58)$$

This frequency f_c is called the cutoff frequency because, for frequencies lower than this, no power will be transmitted down the horn, i.e., the impedance at all positions along the horn is purely reactive. The throat impedance of an infinite hyperbolic horn is plotted in Fig. 9.9.

In Fig. 9.9, the throat impedances for the parabolic, conical, exponential, and hyperbolic horn types are shown. At very high frequencies, all these types behave about alike. At low frequencies, however, there are considerable differences. These differences can be shown by comparison of the throat impedances for the conical and hyperbolic horns with that for the exponential horn.

For all horns, the throat resistance is very low, or zero, below the cutoff frequency. Above the cutoff frequency, the specific throat resistance rises rapidly to its ultimate value of $\rho_0 c$ for those cases where

the rate of taper is *small* near the throat of the horn. For example, the specific throat resistance for the hyperbolic horn reaches $\rho_0 c$ at about one-twentieth the frequency at which the specific throat resistance for the conical horn reaches this value. Similarly for the hyperbolic horn, the specific throat resistance approaches unity at about one-third the frequency for the exponential horn.

It would seem that for best loading conditions on the horn drive unit over the frequency range above the cutoff frequency, one should use the hyperbolic horn. However, it should also be remembered that the nonlinear distortion will be higher for the hyperbolic horn because the wave travels further in the horn before the pressure drops off owing to area increase than is the case for the other horns. For minimum distortion at given power per unit area, the conical horn is obviously the best of the three. The exponential horn is usually a satisfactory compromise in design because it falls between these two extremes.

9.13 FINITE HORNS

Transmission parameters. A horn can be represented as a 2-port network, which is described by the following transmission-parameter matrix:

$$\begin{bmatrix} \tilde{p}_T \\ \tilde{U}_T \end{bmatrix} = \begin{bmatrix} a_{11} & a_{12} \\ a_{21} & a_{22} \end{bmatrix} \cdot \begin{bmatrix} \tilde{p}_M \\ \tilde{U}_M \end{bmatrix} = A \cdot \begin{bmatrix} \tilde{p}_M \\ \tilde{U}_M \end{bmatrix} \quad (9.59)$$

where \tilde{p}_T and \tilde{U}_T are the pressure and volume velocity respectively at the throat and \tilde{p}_M and \tilde{U}_M are the pressure and volume velocity respectively at the mouth. The matrix elements are given by

$$a_{11} = \left. \frac{\tilde{p}_T}{\tilde{p}_M} \right|_{\tilde{U}_M=0} \quad (9.60)$$

$$a_{12} = \left. \frac{\tilde{p}_T}{\tilde{U}_M} \right|_{\tilde{p}_M=0} \quad (9.61)$$

$$a_{21} = \left. \frac{\tilde{U}_T}{\tilde{p}_M} \right|_{\tilde{U}_M=0} \quad (9.62)$$

$$a_{22} = \left. \frac{\tilde{U}_T}{\tilde{U}_M} \right|_{\tilde{p}_M=0} \quad (9.63)$$

Throat impedance. The acoustic impedance at the throat of the horn is given by

$$Z_{AT} = \frac{a_{11}Z_{AM} + a_{12}}{a_{21}Z_{AM} + a_{22}} \quad (9.64)$$

where Z_{AM} is the acoustic radiation impedance at the mouth.

Reverse horn. If the horn is used in reverse, as a tapered transmission line for example, we write

$$\begin{bmatrix} \tilde{p}_M \\ \tilde{U}_M \end{bmatrix} = \frac{1}{\text{Det}(A)} \cdot \begin{bmatrix} a_{22} & a_{12} \\ a_{21} & a_{11} \end{bmatrix} \cdot \begin{bmatrix} \tilde{p}_T \\ \tilde{U}_T \end{bmatrix} \quad (9.65)$$

If no energy is added or dissipated within the horn

$$\text{Det}(A) = a_{11}a_{22} - a_{12}a_{21} = 1 \quad (9.66)$$

However, this does not apply in the case of a transmission line filled with absorbent material.

Finite parabolic horn. The matrix elements are given by

$$a_{11} = -\frac{\pi}{2} kx_M (J_0(kx_T)Y_1(kx_M) - J_1(kx_M)Y_0(kx_T)) \quad (9.67)$$

$$a_{12} = j \frac{\rho_0 c}{S_M} \cdot \frac{\pi}{2} kx_M (J_0(kx_T)Y_0(kx_M) - J_0(kx_M)Y_0(kx_T)) \quad (9.68)$$

$$a_{21} = j \frac{S_T}{\rho_0 c} \cdot \frac{\pi}{2} kx_M (J_1(kx_T)Y_1(kx_M) - J_1(kx_M)Y_1(kx_T)) \quad (9.69)$$

$$a_{22} = \frac{S_T}{S_M} \cdot \frac{\pi}{2} kx_M (J_1(kx_T)Y_0(kx_M) - J_0(kx_M)Y_1(kx_T)) \quad (9.70)$$

where S_T is the area of the throat, S_M is the area of the mouth, and the length l of the horn from the throat to the mouth is given by $l = x_M - x_T$. The throat impedance of a finite parabolic horn is plotted in Fig. 9.10.

Finite conical horn. The matrix elements are given by

$$a_{11} = \sqrt{\frac{S_M}{S_T}} \left(\cos kl - \frac{1}{kx_M} \sin kl \right) \quad (9.71)$$

$$a_{12} = j \frac{\rho_0 c}{\sqrt{S_T S_M}} \sin kl \quad (9.72)$$

$$a_{21} = j \frac{\sqrt{S_T S_M}}{\rho_0 c} \left\{ \left(\frac{1}{kx_M} - \frac{1}{kx_T} \right) \cos kl + \left(1 + \frac{1}{k^2 x_M x_T} \right) \sin kl \right\} \quad (9.73)$$

$$a_{22} = \sqrt{\frac{S_T}{S_M}} \left(\cos kl + \frac{1}{kx_T} \sin kl \right) \quad (9.74)$$

where S_T is the area of the throat, S_M is the area of the mouth, and the length l of the horn from the throat to the mouth is given by $l = x_M - x_T$. The throat impedance of a finite conical horn is plotted in Fig. 9.10.

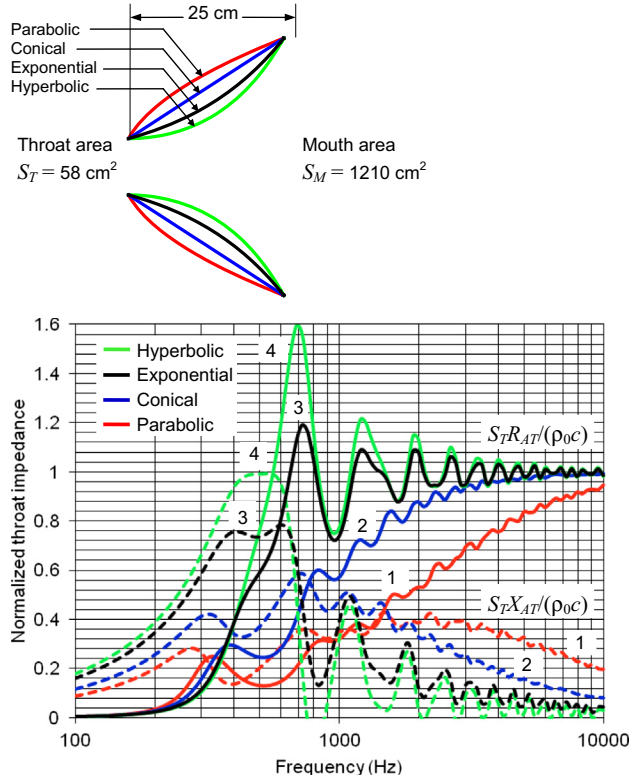


FIG. 9.10 Plot of normalized throat impedances for finite parabolic (1), conical (2), exponential (3), and hyperbolic (4) horns using Eq. (9.64) and Eq. (13.116) for $Z_{AM} = Z_s/S_M$, assuming termination in an infinite baffle.

Real impedances $S_T R_{AT}/(\rho_0 c)$ are represented by solid curves and the imaginary impedances $S_T X_{AT}/(\rho_0 c)$ are represented by dashed curves. The value of α for the hyperbolic horn is $1/2$. The cutoff frequencies of the parabolic, conical, exponential, and hyperbolic horns are 1182 Hz, 792 Hz, 337 Hz, and 399 Hz respectively.

Finite exponential horn [13]. The matrix elements are given by

$$a_{11} = \sqrt{\frac{S_M}{S_T}} (\cos(kl \cos \theta) - \tan \theta \sin(kl \cos \theta)) \quad (9.75)$$

$$a_{12} = j \frac{\rho_0 c}{\sqrt{S_T S_M}} \sec \theta \sin(kl \cos \theta) \quad (9.76)$$

$$a_{21} = j \frac{\sqrt{S_T S_M}}{\rho_0 c} \sec \theta \sin(kl \cos \theta) \quad (9.77)$$

$$a_{22} = \sqrt{\frac{S_T}{S_M}} (\cos(kl \cos \theta) + \tan \theta \sin(kl \cos \theta)) \quad (9.78)$$

where S_T is the area of the throat, $S_M = S_T e^{ml}$ is the area of the mouth, l is the length of the horn from the throat to the mouth, and $\theta = \arcsin(m/2k)$. The throat impedance of a finite exponential horn is plotted in Fig. 9.10.

Finite hyperbolic horn. The matrix elements are given by

$$a_{11} = \sqrt{\frac{S_M}{S_T}} (\cos(kl \cos \theta) - \beta \tan \theta \sin(kl \cos \theta)) \quad (9.79)$$

$$a_{12} = j \frac{\rho_0 c}{\sqrt{S_T S_M}} \sec \theta \sin(kl \cos \theta) \quad (9.80)$$

$$a_{21} = j \frac{\sqrt{S_T S_M}}{\rho_0 c} ((\beta - \alpha) \sin \theta \cos(kl \cos \theta) + (1 + (\alpha\beta - 1) \sin^2 \theta) \sec \theta \sin(kl \cos \theta)) \quad (9.81)$$

$$a_{22} = \sqrt{\frac{S_T}{S_M}} (\cos(kl \cos \theta) + \alpha \tan \theta \sin(kl \cos \theta)) \quad (9.82)$$

where S_T is the area of the throat,

$$S_M = S_T (\cosh(l/x_T) + \alpha \sinh(l/x_T))^2$$

is the area of the mouth, l is the length of the horn from the throat to the mouth, and $\theta = \arcsin(1/kx_T)$. The quantity β is given by

$$\beta = \sqrt{\frac{S_T}{S_M}} (\sinh(l/x_T) + \alpha \cosh(l/x_T)) \quad (9.83)$$

The throat impedance of a finite hyperbolic horn is plotted in Fig. 9.10.

Truncation effects. Whenever the bell diameter is not large or when the horn length is short, it is not possible to use the infinite approximation for the throat impedance. Instead we must use the exact equation of Eq. (9.64). However, we see from Fig. 9.10 that, for a given size horn, the parabolic and conical horns are closer to the infinite ideal of Fig. 9.9 than are the exponential and hyperbolic types. To illustrate what the words “large bell diameter” and “long length” mean, let us refer to Fig. 9.11 for a finite exponential horn of various sizes.

If the circumference of the mouth of the horn divided by the wavelength is less than about 0.5 (i.e., the diameter of the mouth divided by the wavelength is less than about 0.16), the horn will resonate like a cylindrical tube, i.e., at multiples of that frequency where the length is equal to a half wavelength. This condition is shown clearly by the two lower-frequency resonances in Fig. 9.11a.

When the circumference of the mouth of the horn divided by the wavelength is greater than about 3 (i.e., diameter divided by wavelength greater than about 1.0), the horn acts nearly like an infinite horn. This is shown clearly by comparison of c and d of Fig. 9.11, for the region where f/f_c is greater than about 2, which is the case where the ratio of mouth diameter to wavelength exceeds 0.5.

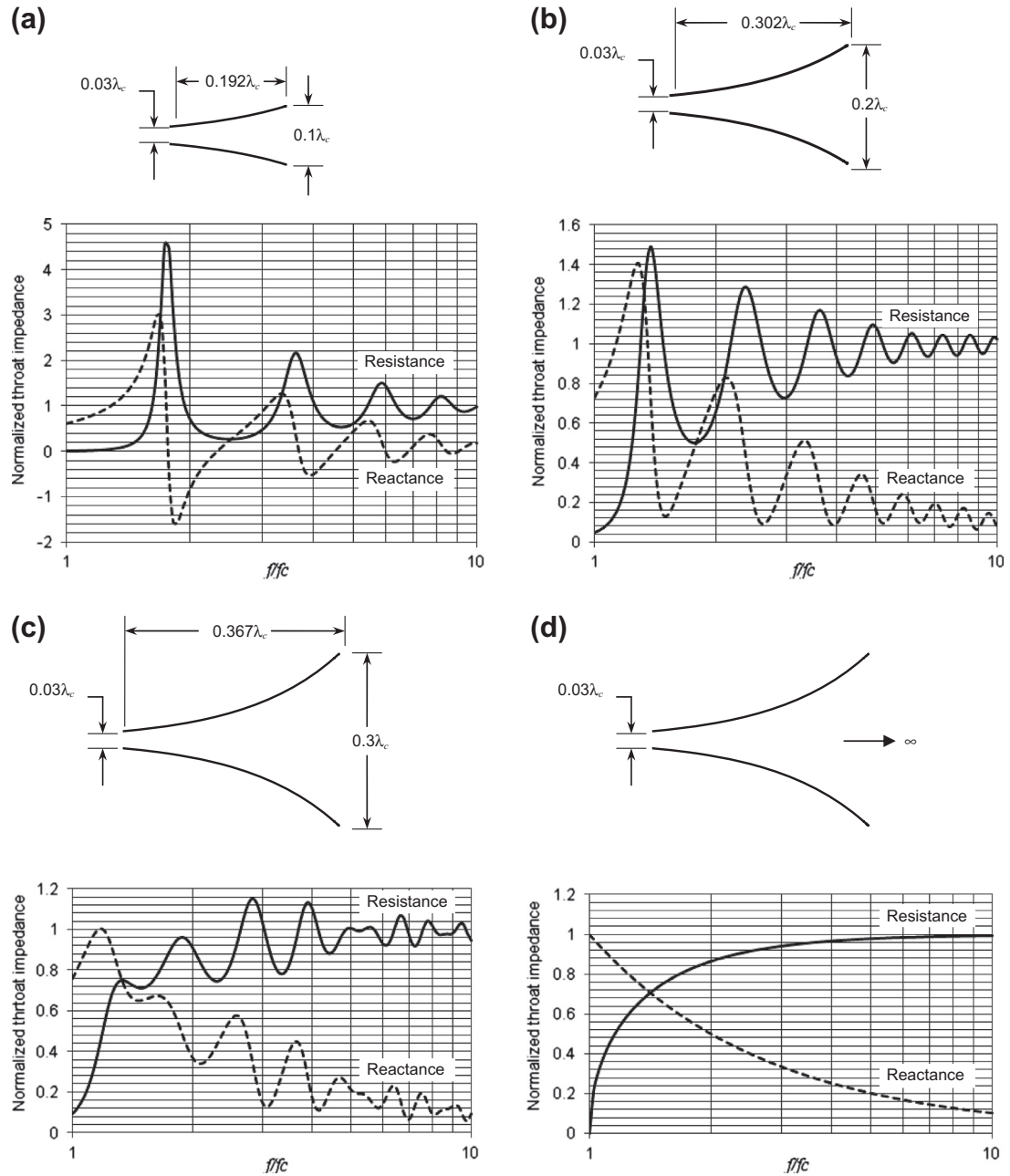


FIG. 9.11 Graphs showing the variation in specific acoustic impedance at the throat of four exponential horns as a function of frequency with bell diameter as the parameter.

The cutoff frequency $f_c = mc/4\pi$ and the throat diameter $= 0.03 c/f_c$; both are held constant. Bell circumferences are (a) $C = 0.314\lambda_c$, (b) $C = 0.628\lambda_c$, (c) $C = 0.942\lambda_c$, and (d) $C = \infty$. The mouth of the horn is assumed to be terminated in an infinite baffle.

In the frequency region where the circumference of the mouth to wavelength ratio lies between about 1 and 3, the exact equation for a finite exponential horn [Eq. (3.49)] must be used, or the results may be estimated from a and b of Fig. 9.11.

When the length of the horn becomes less than one-quarter wavelength, it may be treated as a simple discontinuity of area such as was discussed in Sec. 4.8(pp. 131 to 133).

Obviously, if one chooses a certain mouth area and a throat area to obtain maximum efficiency, the length of the horn is automatically set by the flare constant m , which is in turn directly dependent upon the desired cutoff frequency.

Nonlinear distortion. A sound wave produces an expansion and a compression of the air in which it is traveling. We find from Eq. (2.6) that the relation between the pressure and the volume of a small “box” of the air at 20°C through which a sound wave is passing is

$$P = \frac{0.726}{V^{1.4}} \quad (9.84)$$

where

V is specific volume of air in $\text{m}^3/\text{kg} = 1/\rho_0$

P is absolute pressure in bars, where $1 \text{ bar} = 10^5 \text{ Pa}$

This equation is plotted as curve AB in Fig. 9.12

Assuming that the displacement of the diaphragm of the drive unit is sinusoidal, it acts to change the volume of air near it sinusoidally. For large changes in volume, the pressure built up in the throat of the horn is no longer sinusoidal, as can be seen from Fig. 9.12. The pressure wave so generated travels away from the throat toward the mouth.

If the horn were simply a long cylindrical pipe, the distortion would increase the farther the wave progressed according to the formula (air assumed) [14,15]

$$\frac{p_2}{p_1} = \frac{\gamma + 1}{2\sqrt{2}\gamma} k \frac{p_1}{P_0} x = 1.21k \frac{p_1}{P_0} x \quad (9.85)$$

where

p_1 is rms sound pressure of the fundamental frequency in Pa.

p_2 is rms sound pressure of the second harmonic in Pa.

P_0 is atmospheric pressure in Pa.

$k = \omega/c = 2\pi/\lambda$ is wave number in m^{-1} .

$\gamma = 1.4$ for air.

x is distance the wave has traveled along the cylindrical tube in m.

Equation (9.85) breaks down when the second-harmonic distortion becomes large, and a more complicated expression, not given here, must be used.

In the case of an exponential horn, the amplitude of the fundamental decreases as the wave travels away from the throat, so that the second-harmonic distortion does not increase linearly with distance. Near the throat it increases about that given by Eq. (9.85), but near the mouth the pressure amplitude of the fundamental is usually so low that very little additional distortion occurs.

The distortion introduced into a sound wave after it has traveled a distance x down an exponential horn for the case of a constant power supplied to unit area of the throat is found as follows.

Differentiate both sides of Eq. (9.85) with respect to x , so as to obtain the rate of change in p_2 with x for a constant p_1 . Call this equation (9.85a).

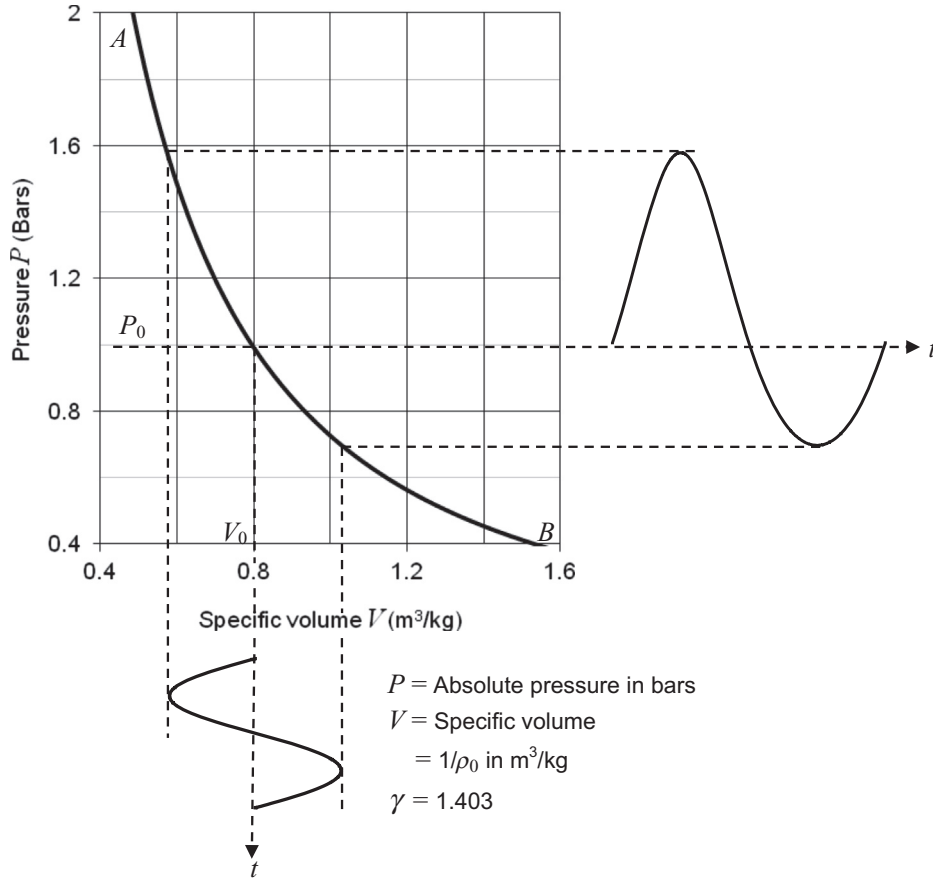


FIG. 9.12 Plot of the gas equation $PV^\gamma = 1.26 \times 10^4$, valid at 20°C.

Normal atmospheric pressure (0.76 m Hg) is shown as $P_0 = 1$ bar.

In Eq. (9.85a), substitute for p_1 the pressure $p_T e^{-mx/2}$, where p_T is the rms pressure of the fundamental at the throat of the horn in Pa and m is the flare constant.

Then let $p_T = \sqrt{I_T \rho_0 c}$, where I_T is the intensity of the sound at the throat in W/m^2 and $\rho_0 c$ is the characteristic acoustic impedance of air in rayls.

Integrate both sides of the resulting equation with respect to x .

This yields:

per cent second-harmonic distortion

$$= \frac{50(\gamma + 1)}{\gamma P_0} \sqrt{\frac{I_T \rho_0 c}{2}} \frac{f}{f_c} (1 - e^{-mx/2}) \quad (9.86)$$

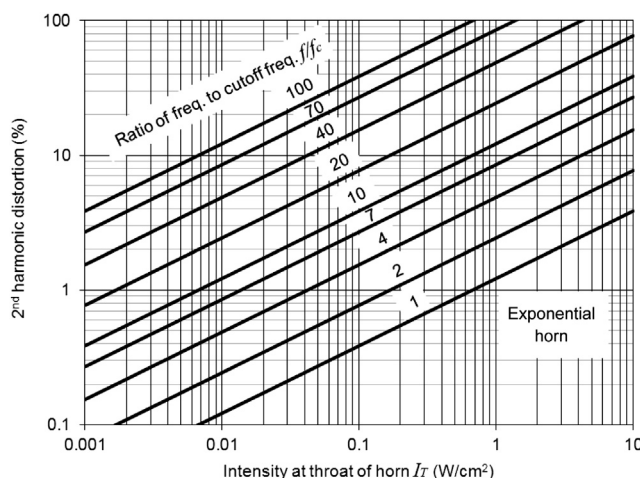


FIG. 9.13 Percentage second-harmonic distortion in an exponential horn as a function of the intensity at the horn throat with the ratio of the frequency to the cutoff frequency as parameter.

For an infinitely long exponential horn, at normal atmospheric pressure and temperature, the equation for the total distortion introduced into a wave that starts off sinusoidally at the throat is

$$\text{Per cent second-harmonic distortion} = 1.22 \frac{f}{f_c} \sqrt{I_T} \times 10^{-2} \quad (9.87)$$

where

f is driving frequency in Hz.

f_c is cutoff frequency in Hz.

I_T is intensity in W/m^2 at the throat of the horn

Equation (9.87) is shown plotted in Fig. 9.13. Actually, this equation is nearly correct for finite horns because most of the distortion occurs near the throat.

Equation (9.87) reveals that, for minimum distortion, the cutoff frequency f_c should be as large as possible, which in turn means as large a flare constant as possible. In other words, the horn should flare out rapidly in order to reduce the intensity rapidly as one travels along the horn toward the mouth.

Unfortunately, a high cutoff frequency is not a feasible solution for horns that are designed to operate over a wide frequency range. In this case, it is necessary to operate the horn at low power at the higher frequencies if the distortion is to be low at these frequencies. This goal is achieved automatically to some extent in reproducing speech and music, because above 1000 Hz the intensity for these sounds decreases by about a factor of 10 for each doubling of frequency.

9.14 BENDS IN HORNS

A horn loudspeaker for use at low frequencies is very large and long, because the flare rate m must be small for a low cutoff frequency and the area of the mouth must be large to radiate sound properly. As

a consequence, it has become popular to “fold” the horn so that it will fit conveniently into a cabinet of reasonable size.

Many types of folded horns have been devised that are more or less successful in reproducing music and speech with satisfactory frequency response. In order to be successful, the bends in folded horns must not be sharp when their lateral dimensions approach a half wavelength, or they will change the spectrum of the radiated sound.

Good data on the comparative performance of folded horns are not available. This is partly because it is difficult to measure the response of large folded horns in an anechoic chamber and partly because commercial companies guard their data. To get some idea of the effect of an abrupt 180° bend as shown in Fig. 9.14, we can use the 2-port model for a cavity developed in Sec. 7.18. The 2-port model is shown in Fig. 9.15. The volume velocity entering the bend is \tilde{U}_{in} and the volume velocity leaving the bend is \tilde{U}_{out} . We assume that the two ducts which are joined at the bend are both infinitely long so that the acoustic source and termination impedances, z_S and z_T respectively, of the network are given by

$$z_S = z_T = \frac{\rho_0 c}{l_x l} \quad (9.88)$$

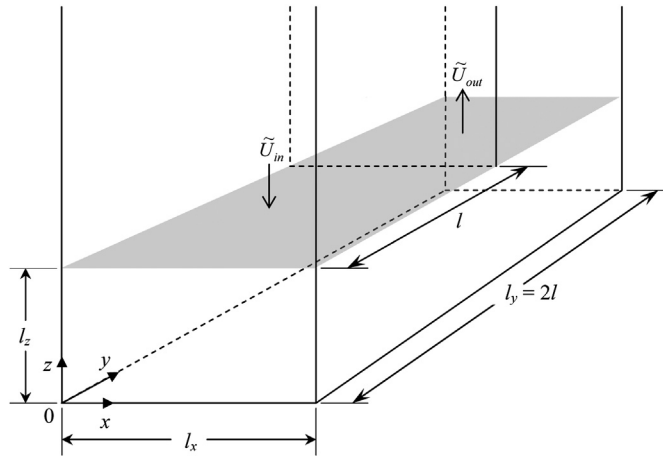


FIG. 9.14 Geometry of 180° bend.

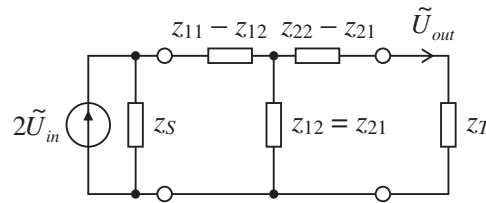


FIG. 9.15 Equivalent electrical circuit for a 180° bend.

The self impedances of the network are

$$z_{11} = z_{22} = -j \frac{\rho_0 c}{l_x l} \left(\frac{\cot kl_z}{2} + kl \sum_{n=0}^{\infty} \frac{\cot \left(\sqrt{k^2 l^2 - \left(n + \frac{1}{2}\right)^2 \pi^2 l_z / l} \right)}{\left(n + \frac{1}{2}\right)^2 \pi^2 \sqrt{k^2 l^2 - \left(n + \frac{1}{2}\right)^2 \pi^2}} \right) \quad (9.89)$$

and the mutual impedances are

$$z_{12} = z_{21} = -j \frac{\rho_0 c}{l_x l} \left(\frac{\cot kl_z}{2} - kl \sum_{n=0}^{\infty} \frac{\cot \left(\sqrt{k^2 l^2 - \left(n + \frac{1}{2}\right)^2 \pi^2 l_z / l} \right)}{\left(n + \frac{1}{2}\right)^2 \pi^2 \sqrt{k^2 l^2 - \left(n + \frac{1}{2}\right)^2 \pi^2}} \right). \quad (9.90)$$

We define the transmission coefficient α by

$$\begin{aligned} \alpha &= 20 \log_{10} \frac{\tilde{U}_{out}}{2\tilde{U}_{in}} \\ &= 20 \log_{10} \frac{z_{12} z_S}{z_{11}^2 - z_{12}^2 + z_{11}(z_S + z_T) + z_S z_T} \end{aligned} \quad (9.91)$$

This is plotted in Fig. 9.16 as a function of kl .

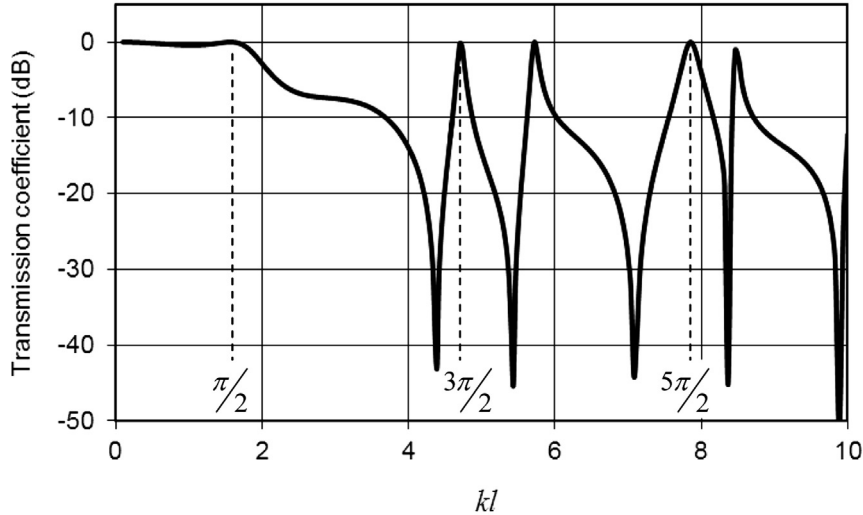


FIG. 9.16 Transmission of sound through a 180° bend as a function of kl .

We see that there are strong transverse modes when

$$kl = (n + 1/2)\pi, \quad n = 0, 1, 2, \dots \quad (9.92)$$

or $2l = (n + 1/2)\lambda$. Such modes of vibration may be reduced by curving the bend or simply by chamfering the corners. If possible, the wavelength should be long compared with the width of the duct at the bend. Then the attenuation will be very small.

We note that this model of the bend does not take into account normal modes resulting from sound reflected back from the bend into the preceding duct because we do not know its length, so we just assume it to be infinite. Supposing we let $z_S = \infty$, we then have a rigid piston with a volume velocity \tilde{U}_{in} where the sound enters the bend at $z = l_z$. This would produce strong normal modes at

$$kl_z = n\pi, \quad n = 1, 2, \dots \quad (9.93)$$

However, such reflections are also reduced by curving the bend or chamfering the corners.

9.15 CROSS-SECTIONAL SHAPES

Earlier it was stated that the cross-sectional shape of a horn is not too important. This is true provided the lateral dimensions of the horn are not comparable with a wavelength. When the lateral dimensions are large enough, standing waves exist across the duct, similar to the standing waves in a closed end tube. These waves are usually not important in an exponential horn that is circular or square in cross section because, generally, only that section of the horn near the mouth is greater than a half wavelength.

In a rectangular horn that is constructed with two sides parallel and the other two sides varying according to the exponential or hyperbolic law, standing waves may exist between the two parallel walls. These resonances occur at wavelengths that are submultiples of the width of the duct, i.e., at frequencies equal to

$$f = \frac{nc}{2l_x} \quad (9.94)$$

or wavelengths equal to

$$\lambda = \frac{2l_x}{n} \quad (9.95)$$

where n is an integer, that is, 1, 2, 3, 4,

For example, suppose that the width of the horn were 0.5 m. Then resonances (standing waves) would occur at 345, 690, 1034, etc., Hz. At these frequencies, reduced power output generally occurs. In general, the upper frequency limit for operation of a horn should be chosen sufficiently low so that troubles from transverse standing waves are avoided.

9.16 MATERIALS

The material from which a horn is constructed is very important. If the side walls of the horn resonate mechanically at one or more frequencies in the range of operation, “dips” in the power-output curve

will occur. Undamped thin metal is the least desirable material because the horn from which it is made will resonate violently at fairly low frequencies. Heavy metals, covered on the outside with thick mastic material so that mechanical resonances are damped, are much better. A concrete or plaster horn 1 or 2 inch in thickness is best because of its weight and internal damping.

Plywood is commonly used in the construction of large horns. Although it is not as satisfactory as concrete, it gives satisfactory results if its thickness exceeds $\frac{3}{4}$ inch and if it is braced with wooden pieces glued on at frequent, irregular intervals.

Example 9.3. Low-frequency horn design. A horn for radiating low frequencies is required. It is desired that the frequency response be flat between 40 and 600 Hz and that the horn be designed to be heard throughout a 500-seat auditorium with a volume of 5000 m³. Therefore, from Fig. 10.17, we see that we need to radiate an acoustic power of 3.6 W if we wish to reproduce the sound of a large orchestra. We shall select the exponential horn as the best compromise shape of horn for our use. Because the lowest frequency at which good radiation is desired is 40 Hz, we choose the mouth area from Eq. (9.24).

$$\text{Mouth area } S_M = \frac{\lambda^2}{4\pi} = \frac{c^2}{4\pi f^2} = 6.05 \text{ m}^2$$

This is probably too large a mouth area for most applications, so that a compromise in design is necessary.

Let us choose arbitrarily a mouth area of 2.4 m². This corresponds to the bell opening shown in Fig. 9.11b. We see from this chart that below $f = 3f_c$, there will be two resonances that are not desirable, but they are fairly well damped.

Let us design for a cutoff frequency of

$$f_c = 40 \text{ Hz}$$

The flare constant m equals [see Eq. (9.49)]

$$m = \frac{4\pi f_c}{c} = \frac{4\pi \times 40}{344.8} = 1.44 \text{ m}^{-1}$$

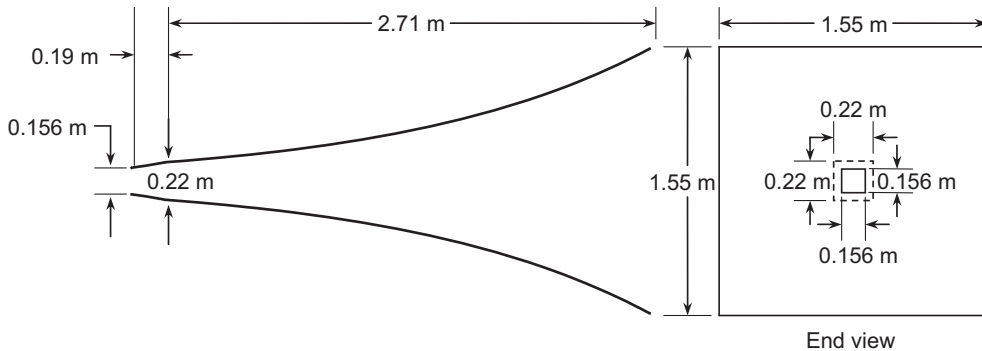


FIG. 9.17 Plans for a simple straight exponential horn with a cutoff frequency of 40 Hz, a throat area of 0.0243 m², and a mouth area of 2.4 m².

Let us choose a 12-inch direct-radiator unit with the following Thiele–Small parameters:

$$\begin{aligned} R_E &= 6 \, \Omega \\ Q_{ES} &= 0.2 \\ Q_{MS} &= 4.4 \\ f_S &= 20 \, \text{Hz} \\ S_D &= 0.0486 \, \text{m}^2 \\ V_{AS} &= 0.368 \, \text{m}^3. \end{aligned}$$

From Eq. (9.9), it appears that for maximum efficiency S_D/S_T should equal $1^{2/3}$. However, to keep the length down, let us make

$$\frac{S_D}{S_T} = 1$$

Then,

$$G_{MT} = \frac{S_T}{\rho_0 c S_D^2} = \frac{1}{1.18 \times 348.8 \times 0.0486} = 0.05 \, \text{m} \cdot \text{N}^{-1} \cdot \text{s}^{-1}$$

Let us calculate the reference efficiency. From Eq. (9.8),

$$E_{ff} = \frac{100 \times 0.05 \times 348.8}{2 \times (0.05 \times 348.8 + 2 \times 2\pi \times 20 \times 0.2 \times 0.368)} = 23.9\%$$

As a trial, let us make $S_D/S_T = 2.0$. Then $G_{MT} = 0.025$, and $E_{ff} = 25.3\%$. Finally, let $S_T/S_D = 2$. Then, $G_{MT} = 0.1$, and $E_{ff} = 18.3\%$.

It is seen that the ratio of the throat and diaphragm areas may be made equal with little loss of efficiency, thereby making our horn of reasonably short length. However, for good high frequency response, it is desirable to have as small a throat area as possible. In order to reconcile this, we shall employ a “rubber neck” [16] which is a short section of horn with a higher flare rate than the rest of the horn (see Fig. 4.10). At low frequencies it behaves as a simple discontinuity so that the throat area is that of the mouth of the neck, but at high frequencies it is that of the throat of the neck. Hence we shall make the area of the mouth of the neck equal to S_D , but the throat area of the neck will be equal to $S_D/2$. Let the neck have a cut-off frequency of 100 Hz. Then its flare constant is

$$m_n = \frac{4\pi f_n}{c} = \frac{4\pi \times 100}{344.8} = 3.65 \, \text{m}^{-1}$$

The length of the neck x_n is found from Eq. (9.39):

$$e^{m_n x_n} = 2$$

or

$$m_n x_n = \ln(2) = 0.693$$

$$x_n = \frac{0.693}{3.65} = 0.19 \, \text{m}$$

The length of the rest of our horn is found from Eq. (9.39):

$$e^{mx} = \frac{2.4}{0.0486} = 49.4$$

or

$$mx = \ln(49.4) = 3.90$$

$$x = \frac{3.90}{1.44} = 2.71 \text{ m}$$

The intensity for a horn with a throat area of $0.5 \times 0.0486 \text{ m}^2$ radiating 3.6 W of acoustic power is 0.015 W/cm^2 , assuming uniform pressure distribution. Let us set the upper limit of operation at 600 Hz. Then $ff_c = 10$. The line for 10 in Fig. 9.13 at 0.015 W/cm^2 shows that the per cent second-harmonic distortion in the horn will be about 1.5%, which, bearing in mind that this is for peaks of short duration, will hardly be audible.

This calculation would seem to indicate that the low-frequency unit could be operated successfully above 600 Hz. However, it seems from experience that for psychological reasons the crossover from the low-frequency to the high-frequency horn should occur at a frequency below 600 Hz for best auditory results.

Let us see what back enclosure volume V_B the drive-unit circuit ought to have if the total compliance C_{M2} is to balance out the mass reactance of the horn at frequencies below the diaphragm resonance frequency. The quantity C_{M2} includes the combined compliance of the loudspeaker C_{MS} and that of the enclosure behind it C_{MB} . From Eqs. (9.17), (9.18), and (9.45), we have the condition

$$\frac{1}{C_{M2}} = \frac{S_D^2}{S_T^2 C_{MT}} = \frac{S_D^2 \rho_0 c^2 m}{2S_T}$$

where

$$\frac{1}{C_{M2}} = \frac{1}{C_{MB}} + \frac{1}{C_{MS}} = \frac{S_D^2 \rho_0 c^2}{V_B} + \frac{S_D^2 \rho_0 c^2}{V_{AS}}$$

so that after canceling all the $S_D^2 \rho_0 c^2$ terms we have

$$V_B = \left(\frac{m}{2S_T} - \frac{1}{V_{AS}} \right)^{-1} = \left(\frac{1.44}{2 \times 0.0486} - \frac{1}{0.368} \right)^{-1} = 0.0826 \text{ m}^3 \text{ or } 82.6 \text{ L}$$

Two possible horns for our design are the straight square horn shown in Fig. 9.17 or the folded horn of the Klipsch type [17] shown in Fig. 9.18, which has the dimensions given in Table 9.1.

By placing the Klipsch horn in the corner of the room, the three adjoining walls form the final part of the horn flare. Of course, this is not the only way to fold a horn [18]. If the straight horn is used, it will probably be necessary to put it partially above the ceiling or below the floor in order to make its presence non-objectionable in the room.

Example 9.4. High-frequency horn design. In this example we shall design a horn loaded tweeter for use with the bass-reflex loudspeaker design of Example 7.3. The tweeter will be the same type as that used for the closed-box design of Example 7.2 and for which a crossover is designed in Example 7.4.

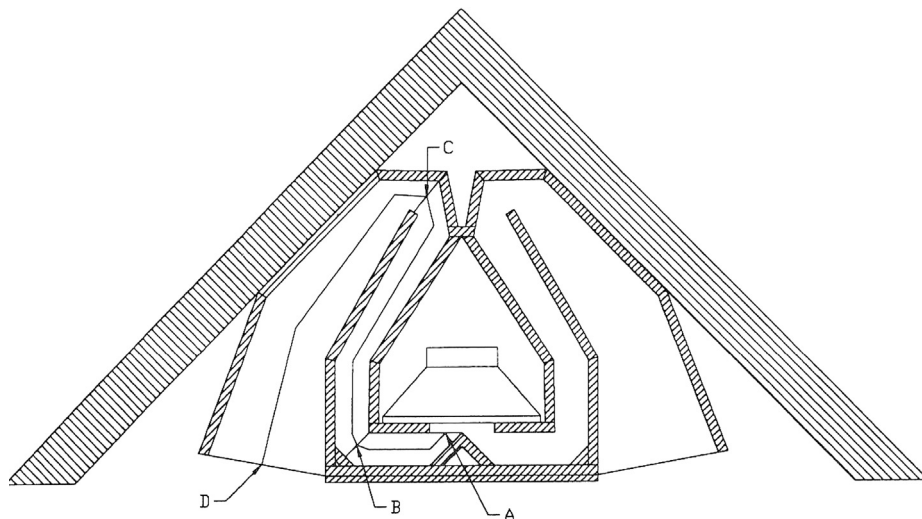


FIG. 9.18 Horizontal section for a Klipsch type of folded exponential horn.

This particular horn is about 1 m high and has smooth response below 600 Hz. There are two 12-inch drive units, one above the other.

Table 9.1 Dimensions of horn in Example 9.3

Location	Length (m)	Area of horn (m ²)	Flare rate (Hz)
Point A	0	0.029	0
Point B	0.209	0.061	97
Point C	0.741	0.075	35
Point C	1.402	0.232	40

However, because the bass-reflex design uses two bass drive units, we shall design a horn for the tweeter in order to increase its sensitivity. The horn, which is shown in Fig. 9.19, is mounted in a sphere so that we can model the radiation from the mouth as a rectangular cap in a sphere, which will be described in detail in Chapter 12. The horn has conical profile in order to give a smooth response with a gentle roll-off (see Fig. 9.10). This makes it easier to design a simple crossover than in the case of exponential or hyperbolic types, which have more abrupt transitions. Also, its cross-section is rectangular in order to smooth out any deep nulls which would otherwise appear in its on-axis response if it were circular (see Fig. 12.21).

From the manufacturer's data we have

$$R_E = 4.9 \, \Omega$$

$$L_E = 50 \, \mu\text{H}$$

$$f_C = 750 \, \text{Hz}$$

$$M_{MS} = 0.32 \, \text{g}$$

$$S_D = 7 \, \text{cm}^2$$

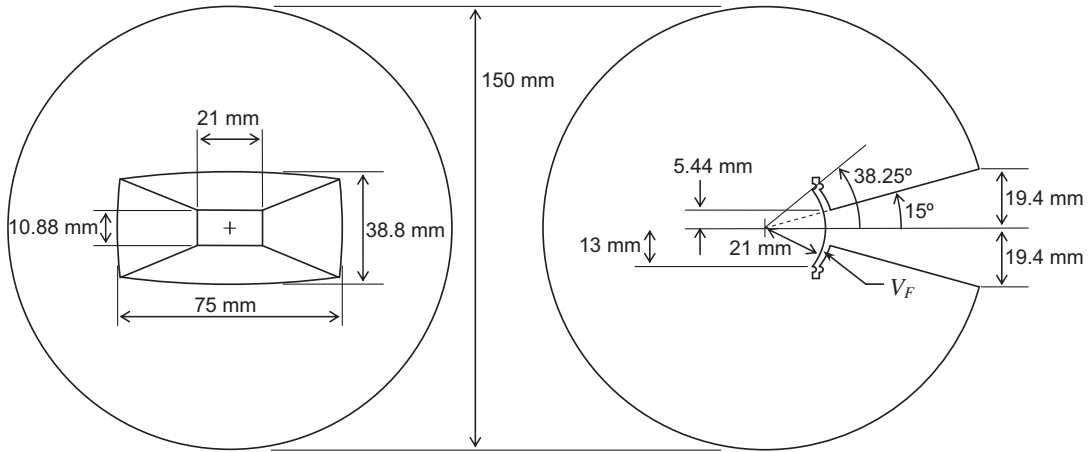


FIG. 9.19 Example of high-frequency horn design. For clarity, only the diaphragm of the drive unit is shown. The front plate, coil and magnet etc. are omitted.

Because the tweeter is supplied with its own integral closed-box enclosure, the resonance frequency f_c is the closed-box resonance frequency. From this we shall deduce the total mechanical compliance C_{MC} , which combines the compliance of the suspension with that of the air in the enclosure. Similarly, the total resistance R_{MC} combines the resistance of the suspension with that of the enclosure. From actual measurements we deduce that

$$Q_{EC} = 0.75$$

$$Q_{MC} = 1.64$$

Also

$$C_{MC} = \frac{1}{(2\pi f_c)^2 M_{MS}} = \frac{10^3}{(2\pi \times 750)^2 \times 0.32} = 0.141 \text{ mm/N}$$

Hence from Eqs. (6.10), (6.11), and (6.12) we obtain

$$Q_{TC} = \frac{Q_{EC} Q_{MC}}{Q_{EC} + Q_{MC}} = 0.515$$

$$R_{MC} = \frac{1}{Q_{MC}} \sqrt{\frac{M_{MS}}{C_{MC}}} = \frac{1}{1.64} \sqrt{\frac{0.32}{0.141}} = 0.92 \text{ N}\cdot\text{s/m}$$

$$Bl = \sqrt{\frac{R_E}{Q_{EC}}} \sqrt{\frac{M_{MS}}{C_{MC}}} = \sqrt{\frac{4.9}{0.75}} \sqrt{\frac{0.32}{0.141}} = 3.14 \text{ T}\cdot\text{m}$$

Let us now create a semi-analytical simulation model of the design of Fig. 9.19 using 2-port networks and transmission matrices, as introduced in Sec. 3.10 and Fig. 4.43. The schematic is shown in Fig. 9.20. Although the drive unit part is based on the circuit of Fig. 9.3, a gyrator has been inserted between the electrical elements and the mechanical ones so that the whole circuit is written using the impedance analogy. Also, we have added the horn and horn mouth impedance to the circuit. We are ignoring the generator impedance R_g since in the experimental setup this is negligible compared with R_E . The dashed boxes are lumped-element 2-port networks and the solid boxes are analytical ones. From the schematic we create the transmission matrices required to represent each 2-port network as follows.

1. *Coil.*

$$\begin{bmatrix} \tilde{e}_g \\ \tilde{i}_g \end{bmatrix} = \begin{bmatrix} 1 & Z_E \\ 0 & 1 \end{bmatrix} \cdot \begin{bmatrix} \tilde{e}_1 \\ \tilde{i}_1 \end{bmatrix} = \mathbf{C} \cdot \begin{bmatrix} \tilde{e}_1 \\ \tilde{i}_1 \end{bmatrix}$$

where $Z_E = R_E + j\omega L_E$.

2. *Electro-Mechanical Transduction.*

$$\begin{bmatrix} \tilde{e}_1 \\ \tilde{i}_1 \end{bmatrix} = \begin{bmatrix} 0 & Bl \\ (Bl)^{-1} & 0 \end{bmatrix} \cdot \begin{bmatrix} \tilde{f}_2 \\ \tilde{u}_2 \end{bmatrix} = \mathbf{E} \cdot \begin{bmatrix} \tilde{f}_2 \\ \tilde{u}_2 \end{bmatrix}$$

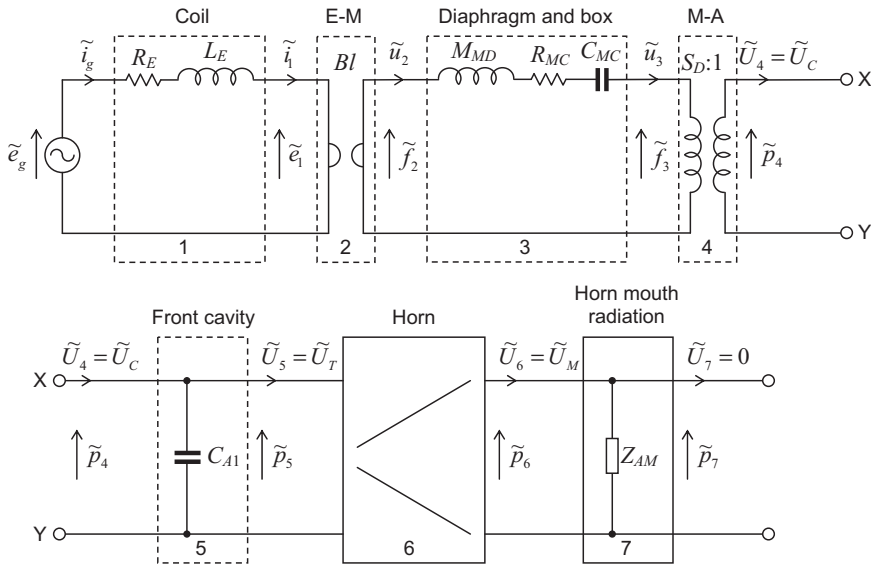


FIG. 9.20 Semi-analytical model of example high-frequency horn design shown in Fig. 9.19 using transmission matrices.

The dashed boxes are lumped-element 2-port networks and the solid boxes are analytical ones.

3. *Diaphragm.*

$$\begin{bmatrix} \tilde{f}_2 \\ \tilde{u}_2 \end{bmatrix} = \begin{bmatrix} 1 & Z_M \\ 0 & 1 \end{bmatrix} \cdot \begin{bmatrix} \tilde{f}_3 \\ \tilde{u}_3 \end{bmatrix} = \mathbf{D} \cdot \begin{bmatrix} \tilde{f}_3 \\ \tilde{u}_3 \end{bmatrix}$$

where $Z_M = j\omega M_{MD} + R_{MC} + 1/(j\omega C_{MC})$. We must exclude the radiation mass from the diaphragm so that

$$M_{MD} = M_{MS} - 16\rho_0 a^3/3, \text{ where } a = \sqrt{S_D/\pi}.$$

4. *Mechano-acoustical transduction.*

$$\begin{bmatrix} \tilde{f}_3 \\ \tilde{u}_3 \end{bmatrix} = \begin{bmatrix} S_D & 0 \\ 0 & S_D^{-1} \end{bmatrix} \cdot \begin{bmatrix} \tilde{p}_4 \\ \tilde{U}_4 \end{bmatrix} = \mathbf{M} \cdot \begin{bmatrix} \tilde{p}_4 \\ \tilde{U}_4 \end{bmatrix}$$

5. *Front cavity.*

$$\begin{bmatrix} \tilde{p}_4 \\ \tilde{U}_4 \end{bmatrix} = \begin{bmatrix} 1 & 0 \\ j\omega C_{A1} & 1 \end{bmatrix} \cdot \begin{bmatrix} \tilde{p}_5 \\ \tilde{U}_5 \end{bmatrix} = \mathbf{F} \cdot \begin{bmatrix} \tilde{p}_5 \\ \tilde{U}_5 \end{bmatrix}$$

where the acoustic compliance of the front cavity, which has a total volume of 1.4 cm^3 , is given by

$$C_{A1} = \frac{V_F}{\rho_0 c^2} = \frac{1.4 \times 10^{-6}}{1.18 \times 344.8^2} = 4.99 \times 10^{-12} \text{ m}^5/\text{N}$$

6. *Horn.*

$$\begin{bmatrix} \tilde{p}_5 \\ \tilde{U}_5 \end{bmatrix} = \begin{bmatrix} b_{11} & b_{12} \\ b_{21} & b_{22} \end{bmatrix} \cdot \begin{bmatrix} \tilde{p}_6 \\ \tilde{U}_6 \end{bmatrix} = \mathbf{H} \cdot \begin{bmatrix} \tilde{p}_6 \\ \tilde{U}_6 \end{bmatrix}$$

where

$$b_{11} = \sqrt{\frac{S_M}{S_T}} \left(\cos kl - \frac{1}{kr_M} \sin kl \right),$$

$$b_{12} = j \frac{\rho_0 c}{\sqrt{S_T S_M}} \sin kl,$$

$$b_{21} = j \frac{\sqrt{S_T S_M}}{\rho_0 c} \left\{ \left(\frac{1}{kr_M} - \frac{1}{kr_T} \right) \cos kl + \left(1 + \frac{1}{k^2 r_M r_T} \right) \sin kl \right\},$$

$$b_{22} = \sqrt{\frac{S_T}{S_M}} \left(\cos kl + \frac{1}{kr_T} \sin kl \right),$$

and $l = r_M - r_T$. We see from Fig. 9.19 that $r_T = 22$ mm and $r_M = 75$ mm. The horn is defined by the angles $\alpha = 15^\circ$ in the vertical direction and $\beta = 30^\circ$ in the horizontal direction. Hence from Eq. (12.69) we can calculate the throat area S_T and mouth area S_M as follows:

$$\begin{aligned} S_T &= 4R_T^2 \left\{ \arctan \left(\frac{\sin \frac{\pi}{12} \sin \frac{\pi}{6}}{1 + \cos \frac{\pi}{12} \sqrt{1 + \sin^2 \frac{\pi}{6}}} \right) + \arctan \left(\frac{\sin \frac{\pi}{12} \sin \frac{\pi}{6}}{1 + \cos \frac{\pi}{6} \sqrt{1 + \sin^2 \frac{\pi}{12}}} \right) \right\} \\ &= 4 \times 0.022^2 \times 0.13 = 2.52 \text{ cm}^2 \\ S_M &= 4 \times 0.075^2 \times 0.13 = 29.3 \text{ cm}^2 \end{aligned}$$

7. Horn Mouth Radiation.

$$\begin{bmatrix} \tilde{p}_6 \\ \tilde{U}_6 \end{bmatrix} = \begin{bmatrix} 1 & 0 \\ Z_{AM}^{-1} & 1 \end{bmatrix} \cdot \begin{bmatrix} \tilde{p}_7 \\ \tilde{U}_7 \end{bmatrix} = \mathbf{R} \cdot \begin{bmatrix} \tilde{p}_7 \\ \tilde{U}_7 \end{bmatrix}$$

The horn mouth radiation impedance Z_{AM} is reasonably well approximated by that of a rectangular cap in a sphere using Eqs. (12.87) and (12.88), where

$$Z_{AM} = (\mathbf{R}_s + jX_s)/S.$$

First we evaluate \tilde{p}_7 at the end of the chain

$$\begin{bmatrix} \tilde{e}_g \\ \tilde{i}_g \end{bmatrix} = \mathbf{A} \cdot \begin{bmatrix} \tilde{p}_7 \\ 0 \end{bmatrix}$$

where

$$\mathbf{A} = \mathbf{C} \cdot \mathbf{E} \cdot \mathbf{D} \cdot \mathbf{M} \cdot \mathbf{F} \cdot \mathbf{H} \cdot \mathbf{R} = \begin{bmatrix} a_{11} & a_{12} \\ a_{21} & a_{22} \end{bmatrix}$$

Hence $\tilde{p}_7 = \tilde{e}_g/a_{11}$. Then we work backwards to obtain the volume velocities we wish to evaluate. In particular, we are interested in the far-field pressure which according to Eq. (12.82) is a function of $\tilde{U}_M = \tilde{U}_6$. This procedure is fairly straightforward and does not involve any matrix inversion. From the mouth radiation matrix (7), we obtain

$$\tilde{U}_M = \tilde{U}_6 = \tilde{p}_7/Z_{AM}$$

In order to plot the normalized far-field on-axis pressure, we simply divide \tilde{U}_M by a reference volume velocity

$$\tilde{U}_{ref} = \frac{\tilde{e}_g B l S_D}{\omega M_{MD} R_E}$$

and multiply it by the on-axis response $D(0, \phi)$ of the spherical cap from Eq. (12.85). A plot of

$$20 \log_{10} \left| D(0, \phi) \tilde{U}_M / \tilde{U}_{ref} \right|$$

is shown in Fig. 9.21. The maximum gain we may expect to see from the horn is $20\log_{10}(S_M/S_T) = 21.3$ dB. However, the actual gain is usually less than this and we see that in this example the combined gain of the horn and baffle effect of the sphere is 14–20 dB between 1.5 kHz and 11 kHz. Finally, we can obtain the input impedance from \tilde{e}_g/\tilde{i}_g where $\tilde{i}_g = a_{21}\tilde{p}_7$ and from above $\tilde{p}_7 = \tilde{e}_g/a_{11}$. Therefore the input impedance is simply $Z_E = a_{11}/a_{21}$, as plotted in Fig. 9.22.

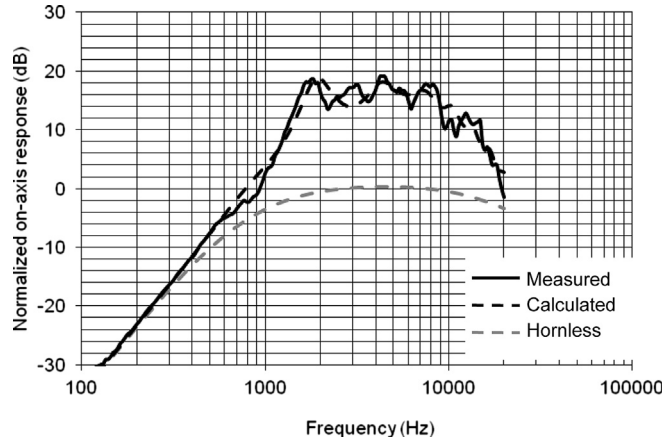


FIG. 9.21 Graphs of the on-axis sound pressure level produced by the high-frequency horn design shown in Fig. 9.19.

The dashed curves are calculated from $20\log_{10}|D(0, \phi)\tilde{U}_M/\tilde{U}_{ref}|$. Solid curves are measured. During testing it was found that placing a small sphere of about 1 cm in diameter in front of the diaphragm improved the correlation between the measured and calculated responses at high frequencies.

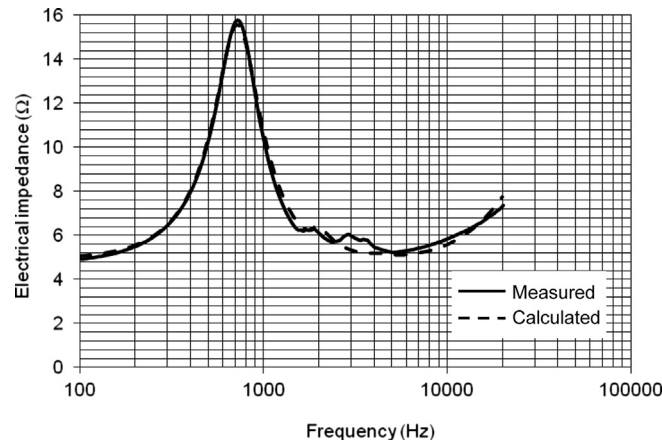


FIG. 9.22 Graphs of the electrical input impedance of the high-frequency horn design shown in Fig. 9.19.

The dashed curves are calculated from $Z_E = |\tilde{e}_g/\tilde{i}_g| = a_{11}/a_{21}$. Solid curves are measured.

References

- [1] An authoritative discussion of horn loudspeakers is found in H. F. Olson. *Elements of Acoustical Engineering*. 2nd ed. New York: D. Van Nostrand Company, Inc.; 1947 Chap. VII.
- [2] Geddes ER, Lee LW. *Audio Transducers*. Michigan: GedLee; 2002. p. 126–63.
- [3] Freehafer JE. The Acoustical Impedance of an Infinite Hyperbolic Horn. *J Acoust Soc Am* 1940;11: 467–76.
- [4] Abramowitz M, Stegun IA. *Handbook of Mathematical Functions*. New York: Dover; 1964. p. 721–69.
- [5] Salmon V. Generalized Plane Wave Horn Theory. *J Acoust Soc Am* 1946;17(3):199–211.
- [6] Martin PA. On Webster's Horn Equation and Some Generalizations. *J Acoust Soc Am* 2004;116(3): 1381–8.
- [7] Hélie T. Unidimensional Models of Acoustic Propagation In Axisymmetric Waveguides. *J Acoust Soc Am* 2003;114(5):2633–47.
- [8] Nederveen CJ, Dalmont J-P. Corrections to the Plane-Wave Approximation in Rapidly Flaring Horns. *Acta Acoust Acust* 2008;94:461–73.
- [9] Fryer PA. Horn Acoustics: Calculation Through the Horn Cutoff Frequency. *J Audio Eng Soc* 2003; 51(1/2):45–51.
- [10] Keele DB. What's so Sacred About Exponential Horns?, in the 51st AES Convention; 1975. paper no. 1038.
- [11] Olson HF, Wolff I. Sound Concentrator for Microphones. *J Acoust Soc Am* 1930;1(3):410–7.
- [12] Salmon V. A New Family of Horns. *J Acoust Soc Am* 1946;17(3):212–8.
- [13] Olson HF. *RCA Review* 1937;1(4):68.
- [14] Thuras AL, Jenkins RT, O'Neil HT. Extraneous Frequencies Generated in Air Carrying Intense Sound Waves. *J Acoust Soc Am* 1935;6:173–80.
- [15] Black LH. A Physical Analysis of the Distortion Produced by the Non-linearity of the Medium. *J Acoust Soc Am* 1940;12:266–7.
- [16] Olson HF. A Horn Consisting of Manifold Exponential Sections. *J Soc Mot Pic Eng* 1938;30(5):511.
- [17] Delgado Jr R, Klipsch PW. A Revised Low-Frequency Horn of Small Dimensions. *J Audio Eng Soc* 2000;48(10):922–9.
- [18] Bright A, Holland K, Fahy FJ. Analysis of a Folded Acoustic Horn. *J Audio Eng Soc* 2004;52(10): 1029–42.
- [19] Dodd M, Oclée-Brown J. New Methodology for the Acoustic Design of Compression Driver Phase Plugs with Concentric Annular Channels. *J Audio Eng Soc* 2009;57(10):771–87.
- [20] Bouwkamp, CJ, Theoretical and numerical treatment of diffraction through a circular aperture, *IEEE Transactions of Antennas and Propagation*, 1970;AP18-2:152–176. This is a translation of his PhD dissertation originally published in Dutch in 1941.
- [21] Webster AG. Acoustical impedance, and the theory of horns and of the phonograph, *Proc Natl Acad Sci U.S.A.* 1919;5:275–82.